Die approbierte Originalversion dieser Diplom-/Masterarbeit ist in der Hauptbibliothek der Technischen Universität Wien aufgestellt und zugänglich.
http://www.ub.tuwien.ac.at

The approved original version of this diploma or master thesis is available at the main library of the Vienna University of Technology.
http://www.ub.tuwien.ac.at/eng

TECHNISCHE UNIVERSITÄT WIEN
Vienna | Austria

Master Thesis

Elemental and Heterogeneity Analysis of Municipal Solid Waste Incineration Fly Ash

Erich Michael Neuwirth B.Sc. (01126996)

Supervisor

Associate Professor Dr. Fumitake Takahashi (Tokyo Institute of Technology)

Ao.Univ.Prof. Dipl.-Ing. Dr.techn. Franz Winter (TU Wien)

Abstract

Municipal solid waste incineration is state-of-the-art process for dealing with waste. However, fly ash contains hazardous compounds like heavy metals and organic pollutants like dioxins. To prevent negative effects on the environment in Japan fly ash is commonly treated with chelating agents to prevent leaching in landfill sites. There are several methods and processes to stabilize fly ashes, however fly ash itself has not been sufficiently characterized. Usually the incineration residues are assumed to be homogeneous. But it may be possible that the heterogeneity of fly ash particles plays an important role on it's leaching behaviour. Therefore this study focuses on characterizing different fly ashes regarding intra- and inter-particle heterogeneity and on the effect of the lime slurry which is injected into flue gas stream for neutralization. It is possible to alter the fly ash particle properties by changing the lime injection point, respectively temperature and the incineration process. In general lime injection has a huge impact on heterogeneity of fly ash particles. Calcium hydroxide leads to more intra-particle homogeneous residues, especially when lime is injected at higher gas temperatures.The samples of different plants are quite different in their results. It seems that incinerated waste also has a huge impact on the composition of MSWI fly ash particles.

Städtische Müll wird standardmäßig in Müllverbrennungsanlagen behandelt. Die Verbrennungrückstände enthalten schädliche bzw. toxische Substanzen wie Dioxine und Schwermetalle. Daher muss bei der Deponierung der Asche besondere Sorgfalt auf deren Behandlung gelegt werden. Grundsätzlich gibt es mehrerer anerkannte Behandlungsmethoden für die Flugasche. In Japan wird aus Platzgründen die Behandlung mit Chelat-Reagenzien bevorzugt eingesetzt. Dabei können aber etwa Schwermetalle heraus gelöst werden. Dies könnte vor allem durch die Heterogenität der Flugsche hervorgerufen werden. Um dieses Ausbleichen der giftigen Substanzen zu verhindern, wird in dieser Studie besonders ein Augenmerk darauf gelegt, die Heterogenität der Flugasche zu untersuchen sowie der Einfluss von Kalkmilch. Dabei wird zwischen inter- und intra-particle Heterogenität unterschieden. Die Ergebnisse zeigen, dass die Flugasche keines Wegs homogen ist und dass man die Heterogenität beeinflussen kann. Gibt man Kalkmilch zu, so sind die Partikel eher homogener. Es ist jedoch zu beachten, dass die inter-partikuläre Heterogenität abnimmt, die intra-partikuläre aber zu nimmt. Ebenfalls nicht zu unterschätzen ist der Beitrag des verbrannten Mülls, der maßgeblich für die Aschezusammensetzung ist.

I, Erich Michael Neuwirth, hereby declare that the work contained in this thesis was carried out by myself during the period 09/2017 – 02/2018. I did not use any other sources than stated in this thesis.

…….....

Ich möchte ganz besonders meinen Eltern danken, die mich immer unterstützt haben und ohne die ich nicht so weit gekommen wäre. Besonderer Dank ergeht auch an meine Schwester, die einen ganz besonderen Platz in meinem Leben einnimmt sowie an all meine Nichten. Diese Arbeit wäre mir auch nicht möglich gewesen ohne der Unterstützung und Betreuung von Prof. Dr. Franz Winter und Prof. Dr. Fumitake Takahashi. Des Weiteren bedanke ich mich bei Herrn Dr. Thomas Rief und beim International Office bzw. jenen Mitarbeitern, die mir das Auslandssemester in Japan ermöglicht haben.

I want to thank my parents for their support and love for all those years. My sister who is a very special person in my life also deserves thanks as well as my nieces. Without the support from Prof. Dr. Franz Winter and Prof. Dr. Fumitake Takahashi this work would not have been possible for me. Furthermore I want to thank Dr. Thomas Rief and the International Office for their support regarding the exchange semester in Japan.

TECHNISCHE
UNIVERSITÄT
WIEN
Vienna | Austria

Master Thesis

Elemental and Heterogeneity Analysis of Municipal Solid Waste Incineration Fly Ash

Erich Michael Neuwirth B.Sc. (01126996)

Supervisor

Associate Professor Dr. Fumitake Takahashi (Tokyo Institute of Technology)

Ao.Univ.Prof. Dipl.-Ing. Dr.techn. Franz Winter (TU Wien)

Index

1Introduction and aim of the thesis....12
2Materials and methods....15
1.1. Municipal solid waste incineration fly ash samples....15
1.2. Elemental analysis....17
3Results and discussion....20
3.1. Inter-particle Heterogeneity....20
I)Untreated fly ash samples....20
Impact of lime injection....20
Impact of gas temperature at lime injection....22
II) Japanese Leaching Test 46 – wet treated fly ash....24
Impact of lime....24
Impact of gas temperature at lime injection....28
III) Toxicity Characteristic Leaching Procedure – mid-part of fly ash particles....32
Impact of lime....32
Impact of gas temperature at lime injection....32
IV)Japanese Leaching Test 19 – core of fly ash particles....37
Impact of lime....37
Impact of gas temperature at lime injection....37
3.2. Intra-particle Heterogeneity....42
I)Untreated fly ash samples....42
Impact of lime injection....42
Impact of gas temperature at lime injection....44
II) Japanese Leaching Test 46 – wet treated fly ash....46
Impact of lime....46
Impact of gas temperature at lime injection....46
III) Toxicity Characteristic Leaching Procedure – mid-part of fly ash particles....51
Impact of lime....51
Impact of gas temperature at lime injection....51
IV)Japanese Leaching Test 19 – core of fly ash particles....56
Impact of lime....56
Impact of gas temperature at lime injection....56
3.3. Single particle analysis vs. bulk analysis....61
3.4. Comparing untreated fly ash samples from different plants....65

4Transition metals and their matrix.....70
5Conclusion.....72
6References.....76

Figure Index

Figure 1.1: Waste generation in Austria, Japan and OECD average since 2000 [6] 13
Figure 1.2: Percentage of municipal solid waste in Austria and Japan used for incineration with energy recovery, recycling, composting and landfill [6].....14
Figure 1.1.1 Typical municipal solid waste incineration plant in Japan with stoker-type incinerator [22].....17
Figure 1.2.1 Area analysis for inter-particle heterogeneity.....19
Figure 1.2.2 Line profile analysis for intra-particle heterogeneity.....19
Figure 1.2.3 step-by-step explanation of area and line analysis and how to get the results.....20
Figure 3.1.1 Major element concentrations on the surface of untreated MSWI fly ash particles. Samples were taken from gas cooling tower. Samples on the left side are without and samples on the right side are with lime injection. µ: average concentration in weight percent. Rsd: relative standard deviation.....22
Figure 3.1.2 Major element concentrations on the surface of untreated MSWI fly ash particles. Samples were taken from gas cooling tower. Samples on the left side are without and samples on the right side are with lime injection. µ: average concentration in weight percent. Rsd: relative standard deviation.....23
Figure 3.1.3 Major element concentrations on the surface of untreated MSWI fly ash particles derived from filter-type dust collector. Lime injection was carried out after for left samples and before gas cooling tower for right samples. µ: average concentration in weight percent. Rsd: relative standard deviation.....24
Figure 3.1.4 Major element concentrations on the surface of untreated MSWI fly ash particles derived from filter-type dust collector. Lime injection was carried out after for left samples and before gas cooling tower for right samples. µ: average concentration in weight percent. Rsd: relative standard deviation.....25
Figure 3.1.5 Comparison of untreated fly ash samples with wet-treated fly ash samples. a) untreated fly ash sample; b) JLT46 wet-treated fly ash sample; 1) sample taken from gas cooling tower with no lime injection; 2) sample taken from gas cooling tower with lime injection before gas cooling tower.....26
Figure 3.1.6 Major element concentrations on the surface of MSWI fly ash particles after JLT46. Samples were taken from gas cooling tower. Samples on the left side are without and samples on the right side are with lime injection. µ: average concentration in weight percent. Rsd: relative standard deviation.....27
Figure 3.1.7 Major element concentrations on the surface of MSWI fly ash particles after JLT46. Samples were taken from gas cooling tower. Samples on the left side are without and samples on the right side are with lime injection. µ: average concentration in weight percent. Rsd: relative standard deviation.....28
Figure 3.1.8 Comparison of untreated fly ash samples with wet-treated fly ash samples. a) untreated fly ash sample; b) JLT46 wet-treated fly ash sample; 1) sample taken from filter-type dust collector with lime injection after gas cooling tower; 2) sample taken from filter-type dust collector with lime injection before gas cooling tower.....30
Figure 3.1.9 Major element concentrations on the surface of untreated MSWI fly ash particles derived from filter-type dust collector after JLT46. Lime injection was carried out after for left samples and before gas cooling tower for right samples. µ: average concentration in weight percent. Rsd: relative standard deviation.....31
Figure 3.1.10 Major element concentrations on the surface of untreated MSWI fly ash particles derived from filter-type dust collector after JLT46. Lime injection was carried out after for left samples and before gas cooling tower for right samples. µ: average concentration in weight percent. Rsd: relative standard deviation.....32
Figure 3.1.11 Major element concentrations of MSWI fly ash particles after TCLP. Samples were taken from gas cooling tower. Samples on the left side are without and samples on the right side are with lime injection. µ: average concentration in weight percent. Rsd: relative standard deviation.....34

Figure 3.1.12 Major element concentrations of MSWI fly ash particles after TCLP. Samples were taken from gas cooling tower. Samples on the left side are without and samples on the right side are with lime injection. μ: average concentration in weight percent. Rsd: relative standard deviation.....35
Figure 3.1.13 Major element concentrations on the surface of MSWI fly ash particles after TCLP. Samples were taken from filter-type dust collector. Lime injection was carried out after for left samples and before gas cooling tower for right samples. μ: average concentration in weight percent. Rsd: relative standard deviation.....36
Figure 3.1.14 Major element concentrations on the surface of MSWI fly ash particles after TCLP. Samples were taken from filter-type dust collector. Lime injection was carried out after for left samples and before gas cooling tower for right samples. μ: average concentration in weight percent. Rsd: relative standard deviation.....37
Figure 3.1.15 Major element concentrations of MSWI fly ash particles after JLT19. Samples were taken from gas cooling tower. Samples on the left side are without and samples on the right side are with lime injection. μ: average concentration in weight percent. Rsd: relative standard deviation.....39
Figure 3.1.16 Major element concentrations of MSWI fly ash particles after JLT19. Samples were taken from gas cooling tower. Samples on the left side are without and samples on the right side are with lime injection. μ: average concentration in weight percent. Rsd: relative standard deviation.....40
Figure 3.1.17 Major element concentrations on the surface of MSWI fly ash particles after JLT19. Samples were taken from filter-type dust collector. Lime injection was carried out after for left samples and before gas cooling tower for right samples. μ: average concentration in weight percent. Rsd: relative standard deviation.....41
Figure 3.1.18 Major element concentrations on the surface of MSWI fly ash particles after JLT19. Samples were taken from filter-type dust collector. Lime injection was carried out after for left samples and before gas cooling tower for right samples. μ: average concentration in weight percent. Rsd: relative standard deviation.....42
Figure 3.2.1 Coefficient of variation of major elements in untreated fly ash samples taken from gas cooling tower. Samples on the left side are without and samples on the right side are with lime injection. Values shown in each figure are average CV values of each element.....43
Figure 3.2.2 Coefficient of variation of major elements in untreated fly ash samples taken from gas cooling tower. Samples on the left side are without and samples on the right side are with lime injection. Values shown in each figure are average CV values of each element.....44
Figure 3.2.3 Major element concentrations on the surface of untreated MSWI fly ash particles derived from filter-type dust collector. Lime injection was carried out after for left samples and before gas cooling tower for right samples. Values shown in each figure are average CV values of each element.....45
Figure 3.2.4 Major element concentrations on the surface of untreated MSWI fly ash particles derived from filter-type dust collector. Lime injection was carried out after for left samples and before gas cooling tower for right samples. Values shown in each figure are average CV values of each element.....46
Figure 3.2.5 Major element concentrations on the surface of MSWI fly ash particles after JLT46. Samples were taken from gas cooling tower. Samples on the left side are without and samples on the right side are with lime injection. Values shown in each figure are average CV values of each element.....48
Figure 3.2.6 Major element concentrations on the surface of MSWI fly ash particles after JLT46. Samples were taken from gas cooling tower. Samples on the left side are without and samples on the right side are with lime injection. Values shown in each figure are average CV values of each element.....49
Figure 3.2.7 Major element concentrations on the surface of MSWI fly ash particles after JLT46. Samples were taken from filter-type dust collector. Lime injection was carried out after for left samples and before gas cooling tower for right samples. Values shown in each figure are average CV values of each element.....50

Figure 3.2.8 Major element concentrations on the surface of MSWI fly ash particles after JLT46. Samples were taken from filter-type dust collector. Lime injection was carried out after for left samples and before gas cooling tower for right samples. Values shown in each figure are average CV values of each element.....51
Figure 3.2.9 Major element concentrations of MSWI fly ash particles after TCLP. Samples were taken from gas cooling tower. Samples on the left side are without and samples on the right side are with lime injection. Values shown in each figure are average CV values of each element.....53
Figure 3.2.10 Major element concentrations of MSWI fly ash particles after TCLP. Samples were taken from gas cooling tower. Samples on the left side are without and samples on the right side are with lime injection. Values shown in each figure are average CV values of each element.....54
Figure 3.2.11 Major element concentrations on the surface of MSWI fly ash particles after TCLP. Samples were taken from filter-type dust collector. Lime injection was carried out after for left samples and before gas cooling tower for right samples. Values shown in each figure are average CV values of each element.....55
Figure 3.2.12 Major element concentrations on the surface of MSWI fly ash particles after TCLP. Samples were taken from filter-type dust collector. Lime injection was carried out after for left samples and before gas cooling tower for right samples. Values shown in each figure are average CV values of each element.....56
Figure 3.2.13 Major element concentrations of MSWI fly ash particles after JLT19. Samples were taken from gas cooling tower. Samples on the left side are without and samples on the right side are with lime injection. Values shown in each figure are average CV values of each element.....58
Figure 3.2.14 Major element concentrations of MSWI fly ash particles after JLT19. Samples were taken from gas cooling tower. Samples on the left side are without and samples on the right side are with lime injection. Values shown in each figure are average CV values of each element.....59
Figure 3.2.15 Major element concentrations of MSWI fly ash particles after JLT19. Samples were taken from filter-type dust collector. Lime injection was carried out after for left samples and before gas cooling tower for right samples. Values shown in each figure are average CV values of each element.....60
Figure 3.2.16 Major element concentrations of MSWI fly ash particles after JLT19. Samples were taken from filter-type dust collector. Lime injection was carried out after for left samples and before gas cooling tower for right samples. Values shown in each figure are average CV values of each element.....61
Figure 3.4.1 Major element concentrations on the surface of untreated MSWI fly ash particles derived from filter-type dust collector. Lime injection was carried out after gas cooling tower for both samples. μ: average concentration in weight percent. rsd: relative standard deviation.....68
Figure 3.4.2 Major element concentrations of untreated MSWI fly ash particles derived from filter-type dust collector. Lime injection was carried out after gas cooling tower for both samples. Values shown in each figure are average coefficients of variation of each element.....69
Figure 3.4.3 Major element concentrations of untreated MSWI fly ash particles derived from filter-type dust collector. Lime injection was carried out after gas cooling tower for both samples. Values shown in each figure are average coefficients of variation of each element.....70

Table Index

Table 1: Leaching test conditions.....17
Table 2: Energy dispersive X-ray fluorescence analysis and comparison with SEM/EDX single particle analysis results of MSWI fly ash taken from gas cooling unit.....64
Table 3: Energy dispersive X-ray fluorescence analysis and comparison with SEM/EDX single particle analysis results of MSWI fly ash taken from air pollution control device.....65
Table 4: Composition of titan and iron rich spots after Japanese Leaching Test 19.....72
Table 5: Composition of zinc rich spots after Japanese Leaching Test 19 and Toxicity Characteristic Leaching Procedure.....72
Table 6: a quantitative summary of inter-particle heterogeneity.....74
Table 7: a quantitative summary of intra-particle heterogeneity.....75

Abbreviations

CV	coefficient of variation
FA	fly ash
HAc	acetic acid
HCl	hydro chloric acid
JLT	Japanese Leaching Test
keV	kilo electron Volt
M	mol/l
MSW(I)	municipal solid waste (incineration)
rsd	relative standard deviation
TCLP	Toxicity Characteristic Leaching Procedure
wt%	weight percentage
ZAF	Z...atomic number, A...absorption, F...fluorescence
μ	average value of weight percentage

1 Introduction and aim of the thesis

In 2015 in Japan 344 kg/capita municipal solid waste (MSW) was produced. This value is relatively low if compared to other OECD countries (520 kg/capita) or Austria (570 kg/capita) as shown in figure 1.1. But in consideration of the population nearly 44,000 kilo tons of waste have to be treated and 468 tons or roughly 1% is deposited in landfill sites. In Japan 78% of MSW is incinerated in mostly stoker-type incinerators and the rest is recycled. In Austria about 5,000 kilo tons of waste have to be treated each year. Almost 40% are incinerated, one third is being composted, one fourth is recycled and the rest is stored in landfill sites [6].

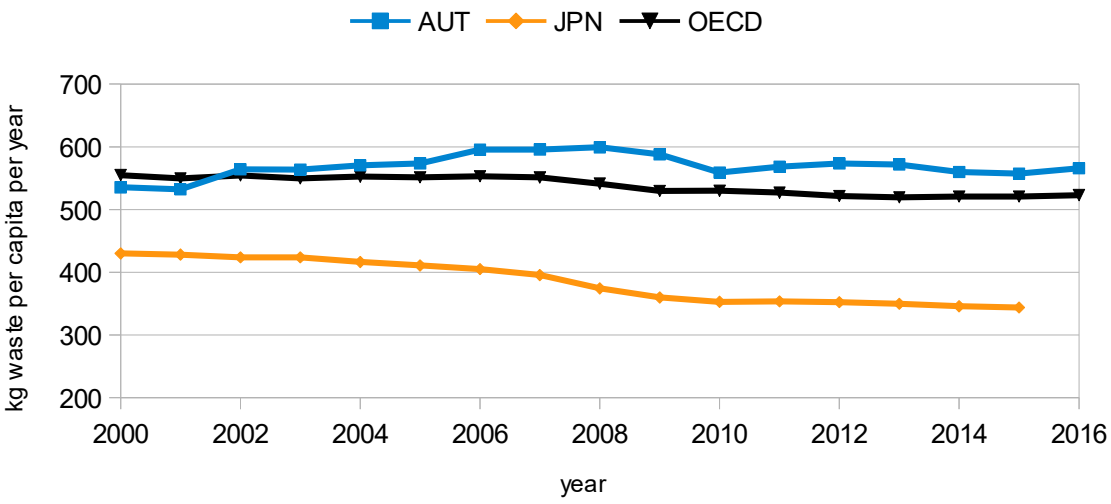

Figure 1.1: Waste generation in Austria, Japan and OECD average since 2000 [6]

The huge advantage of incinerating waste is the reduction of it's volume by 90% and it's weight by 70%. Such incineration plants produce mainly bottom ash but also fly ash as waste. The amount of fly ash generated lies around 3.2wt% of incinerated waste and 9wt% of total ash generated during incineration [4],[16]. For bottom ash there are already processes where the bottom

ash can be used as raw material (e.g. concrete and other building materials) [7],[8]. On the other hand MSW incineration fly ash also has the potential to be used as raw material for other processes which regain zinc and other metals [9],[14].

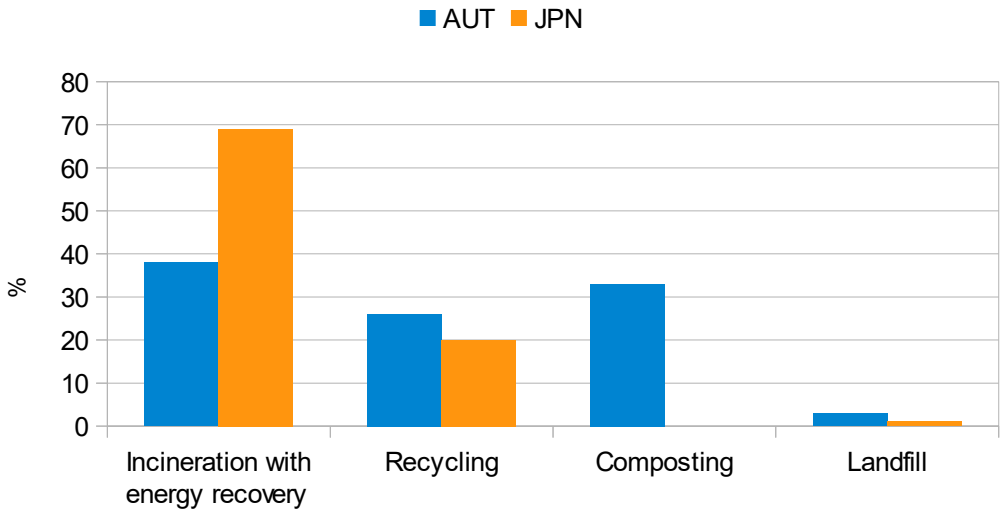

Figure 1.2: Percentage of municipal solid waste in Austria and Japan used for incineration with energy recovery, recycling, composting and landfill [6]

The main problem is still the hazardousness of fly ash due to heavy metals like Hg, Pb, Cd but also Zn, Cu, Fe, Cr and dioxins. That is the reason why fly ash requires special treatment like melting, cementitious stabilization and solidification, stabilization with chelating agent or acid extraction before the waste is disposed of in landfill sites [4]. In Japan MSW incineration fly ash is mainly treated with chemicals like pyrrolidine, imine, carbamate or thiol to control the leaching of especially heavy metals but also of volatile toxic metals and any other potentially toxic compounds. The usage of such chelating agents is not the safest one regarding leaching of metals. But in combination of low required volume in waste disposal, cost effectiveness per ton waste and easy feasibility in already existing processes chelating agents are widely used in Japan. In America bottom ash and fly ash are mixed together and used for cement, concrete and fertilizer. However,

ash pretreatment is still necessary as X. Sun et al. investigated [12]. F. Huber et al. proposed new concepts for fly ash management in Vienna, Austria. They discussed different treatment methods, recycling of certain metals as well as deposition and took cost effectiveness, feasibility and environmental issues into account [11]. The leachability of aforementioned metals is greatly affected by the pH shown by B. Zhang et al. [1], J. Jianguo et al. [3] and F. Jiao [13]. But there are other parameters that have an impact on the leaching behaviour of metals to contribute to secondary pollution of treated fly ash. One parameter which is not paid enough attention to is the heterogeneity of fly ash particles. Generally fly ash is considered as homogeneous although micro-scale observation gave different results as shown by Kitamura et al. They investigated mineralogical surface conversions of MSW fly ash and they showed that there can be great changes on particle surface with formation of secondary minerals [2],[10].

In this study intra- and inter- particle heterogeneity of fly ash particles generated from stoker-type incinerators is observed and compared to previous results. The impact of injected limestone slurry after and before the gas cooling tower into flue gas stream on particle surface, mid-part and core is investigated. Furthermore concentrated spots of transition metals titan, iron and zinc are analysed to identify a possible matrix around those metals. Aforementioned investigations are done in order to understand and interfere with the leaching behaviour of fly ashes.

2 Materials and methods

1.1. Municipal solid waste incineration fly ash samples

The current investigation involved analysation of four untreated fly ash samples. All samples were obtained from one Stoker-type MSWI plant but from two different processes. For both processes fly ash samples were taken from filter-type dust collector and directly from gas cooling tower. For the common process a lime slurry [$Ca(OH)_2$] mixed with activated carbon is injected into flue gas stream in order to absorb acidic flue gases and to adsorb organic pollutants like dioxins and heavy metals. The second point for adding lime is before gas cooling tower. Flue gases enter gas cooling unit with 250°C and at filter-type dust collector a temperature of 160°C is reached. In figure 1.1.1 a flow sheet of the incineration process is shown with highlighted limestone injection points and sample points. Under wet and alkaline conditions secondary minerals like gypsum ($CaSO_4 \cdot 2H_2O$), calcite ($CaCO_3$), calcium chloride ($CaCl_2$) and calcium hydroxide chloride (CaOHCl) will be formed on particle surface. Fly ash samples were dried and analysed with SEM/EDX to determine the heterogeneity of FA particles. Furthermore Japanese Leaching Test 19 and 46, and Toxicity Characteristic Leaching Procedure (TCLP, US EPA Method 1311) were conducted to get more information about water soluble and semi-soluble compounds and about the fly ash core. Regarding JLT19 1M hydrochloric acid is used as a solvent in liquid to solid (L/S) ratio of 33.3 ml/g. The samples are shaken for 2 hours at 200 rpm. Then they are filtrated via 0.45 µm mesh-membrane filter. This leaching test is supposed to dissolute all soluble and semi-soluble components at acidic conditions. The conditions for JLT46 are water as solvent, liquid/solid ratio is 10 ml/g. The shaking time is 6 hours with 200 rpm. The filtration procedure is same with JLT19. JLT46 only water soluble compounds on FA particle surface are dissolved. TCLP aims to solute

soluble and semi-soluble species under weak acidic conditions. Therefore 0.57 v% acetic acid is used as solvent and the L/S ratio is 20 ml/g. The samples are shaken for 18 hours at 30 rpm. Then filtration is done with 0.6-0.8 µm glass fibre filter. However these tests were used to remove soluble and/or semi-soluble compounds only and not for analysing leaching behaviour. Therefore the residues were of interest and after drying at room temperature they were analysed using SEM/EDX.

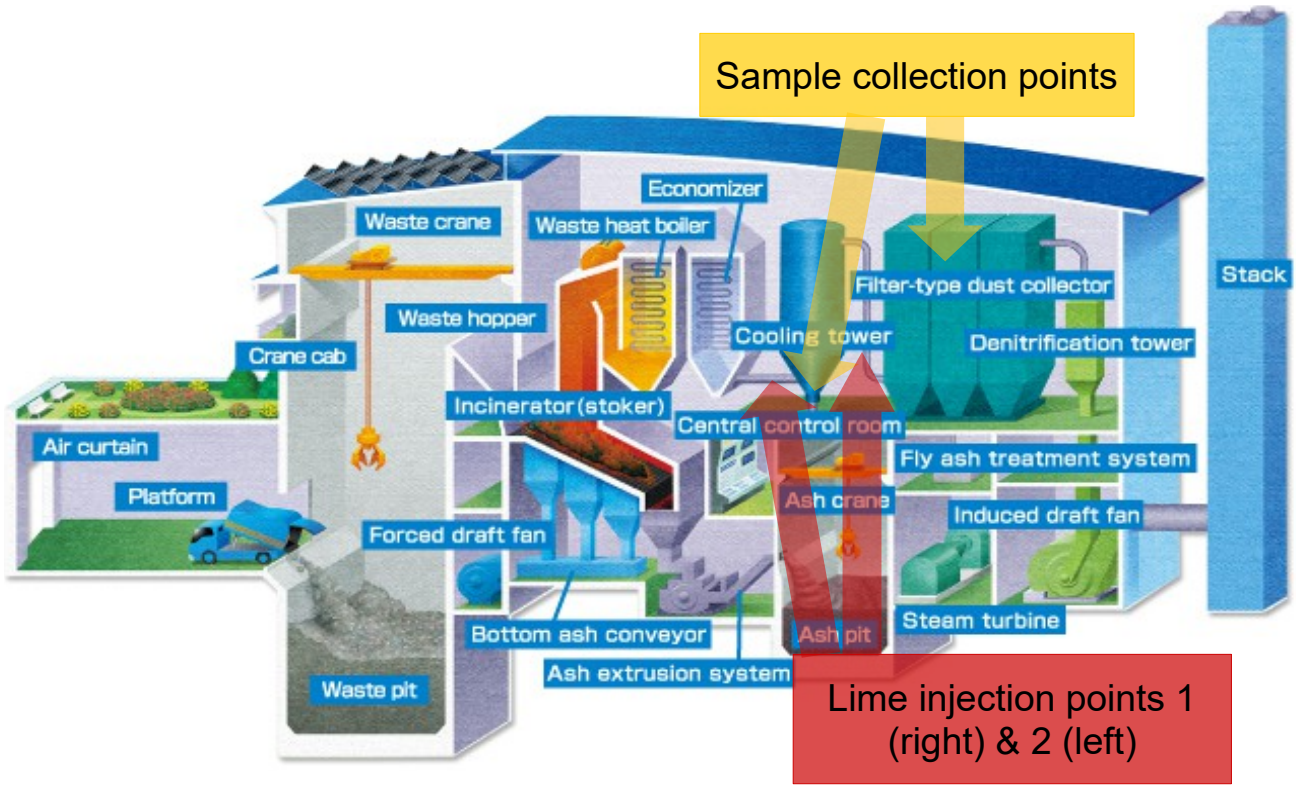

Figure 1.1.1 Typical municipal solid waste incineration plant in Japan with stoker-type incinerator [22]
Source: http://www.takuma.co.jp/english/product/msw/images/stoker_msw/img3.jpg

Table 1: Leaching test conditions

	JLT 19	**JLT 46**	**TCLP**
Solvent	1M hydrochloric acid	Water	0.57 vol% acetic acid
L/S [ml/g]	33.3	10	20
Shaking speed [rpm]	200	200	30
Shaking time [hour]	2	6	18
Filter [µm]	0.45 membrane filter	0.45 membrane filter	0.6-0.8 glass fibre filter

1.2. Elemental analysis

All samples (that includes untreated FA samples as well as all samples obtained from leaching tests) were analysed using secondary electron microscope (SEM: SS-550, Shimadzu Co., Japan/JSM-7600 F, JEOL Ltd., Japan/JSM-6610LA, JEOL Ltd., Japan). To the same equipment an energy dispersive X-ray spectrometer is attached (SEM-EDX: Genesis 2000, EDAX Co., Japan/JED-2300, JEOL Ltd., Japan/EX-94300S4L1Q, JEOL Ltd., Japan). The main focus lies on EDX analysis of sodium (Na), calcium (Ca), aluminium (Al), silicon (Si), potassium (K), magnesium (Mg), chlorine (Cl), sulphur (S), titanium (Ti), iron (Fe) and zinc (Zn). The powdery samples were prepared on double adhesive graphite tape and sputtered with platinum to avoid charge-up effects during SEM observation. It should be noted that Ti, Fe and Zn content is detectable only after conducting leaching tests. Therefore in untreated fly ash samples only the aforementioned first eight elements were analysed. In addition to microscopic investigation also macroscopic element-specific data was gained by energy dispersive X-ray fluorescence spectrometry (S2LANGER/LET BRUKER AXS). By comparing XRF with SEM-EDX data accuracy of microscopic based results can be shown.

Through SEM-EDX obtained data is further processed in order to measure two different types of heterogeneity. In figure 1.2.3 all necessary steps for either analysis method are shown and described. The first type is inter-particle heterogeneity. To obtain weight percentage of certain elements the area of interest – the particle – has to be defined by drawing a line around the particle, as shown in figure 1.2.1. Equation (1) shows the calculation of the average weight percentage of one element for one sample. A quantitative analysis is obtained via ZAF correction and standardless mode. The result of area analysis is weight percentage of observed elements regarding only one particle. Weight percentage of particles is counted in certain margins and divided by the number of

particles investigated (at least 50) to get the relative frequency. Then histograms are drawn for each sample and each element to show distributions, average and relative standard deviation. The second analysis focuses on intra-particle heterogeneity. Via line profile analysis each particle is divided into five parts of same height, as shown in 1.2.2. It should be noted that the whole rectangle should be inside of the particle. The result is a number for each element and each pixel of that rectangular. By calculating one average and one standard deviation over all five rectangles it is possible to describe the intra-particle heterogeneity.

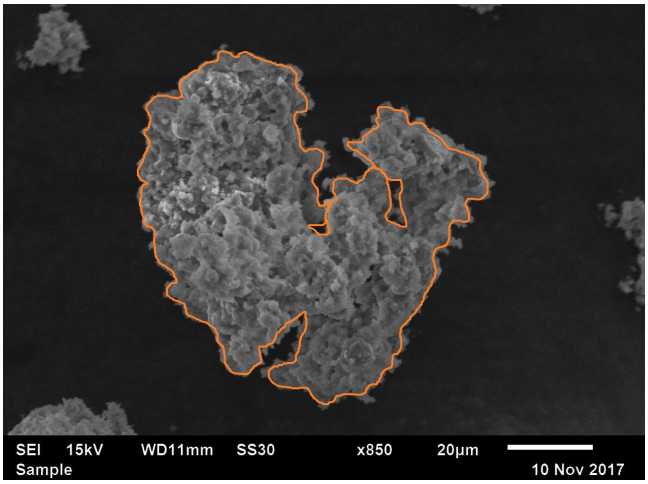

Figure 1.2.1 Area analysis for inter-particle heterogeneity

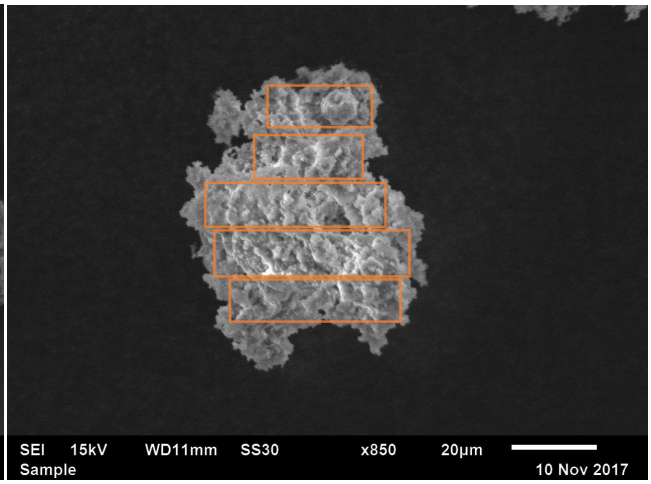

Figure 1.2.2 Line profile analysis for intra-particle heterogeneity

Out of that data one coefficient of variation (CV) for each particle can be calculated by dividing the standard deviation through the average, according to equation (2). Then over all particles of one sample an average CV value can be calculated. A low CV value indicates an equally distributed element throughout the whole particle. On the other hand a high CV value can be obtained from particles in which there are spots of concentrated elements. Results regarding the common process are compared with another fly ash sample from a different Stoker-type MSWI plant to estimate difference between fly ashes.

$$\mu = \sum_{a=1}^{b=50} x_a / b \quad (1)$$

$$Coefficient\ of\ Variation = \frac{standard\ deviation}{average} \quad (2)$$

Area analysis	Line analysis
ZAF method standardless quantitative analysis (settings changeable in the programme)	For each point of the rectangles and each element a numerical value is obtained
↓	↓
for one particle: wt% Na, wt% Cl, wt% Ca, etc.	for one particle: many points with element-specific information
↓	↓
calculating average weight percentage μ and relative standard deviation for each element of one sample	Na: 0.1 1.4 5.2 10.5 0.03 etc. Cl: 10.1 4.8 3.2 0.7 8.6 0.1 etc.
↓	↓
shown in figures: distributions, average weight percentages and relative standard deviations	calculating average and standard deviation using all points of one element of one particle
	↓
	calculating coefficient of variation of each element for one particle
	↓
	calculating overall average coefficient of variation for each element using all particles of one sample
	↓
	shown in figures: distributions of coefficients of variation, overall average coefficient of variation for each element and sample

Figure 1.2.3 step-by-step explanation of area and line analysis and how to get the results

3 Results and discussion

3.1. Inter-particle Heterogeneity

I) Untreated fly ash samples

Impact of lime injection

The average values of weight percentage are higher for all elements except chlorine and calcium if no lime is injected into flue gases. That is in accordance with the occurring reactions. Lime is injected to neutralize acid gases like hydrogen chlorine and therefore the weight percentage of chlorine and calcium should increase. Sulphur decreases slightly although sulphur oxides are also neutralized. This leads to the assumption that the majority of formed species are containing calcium. Regarding inter-particle heterogeneity it seems like lime triggers more heterogeneous fly ash particle surfaces. Only chlorine and sulphur remain almost same and calcium becomes more homogeneous due to lime injection.

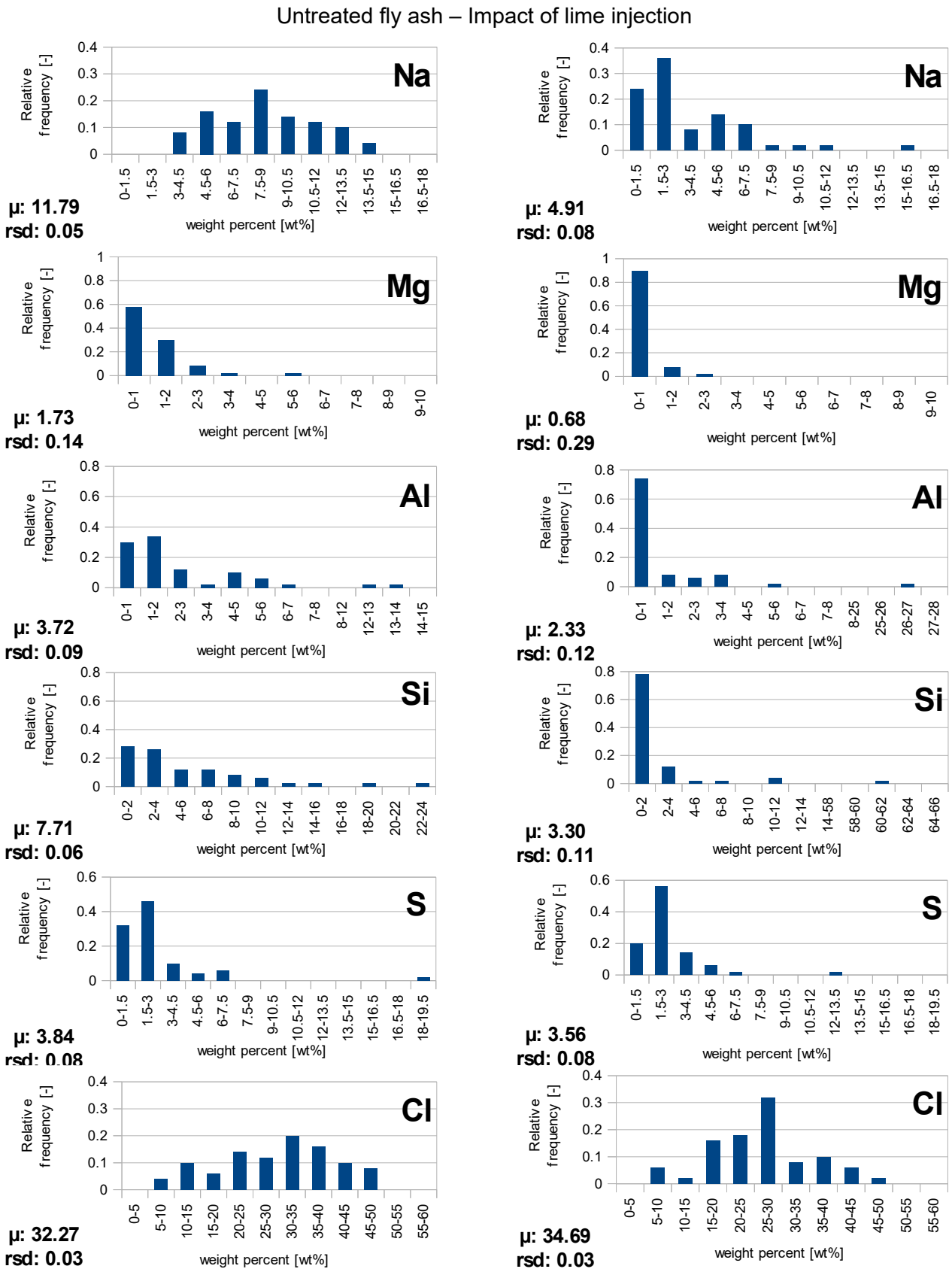

Figure 3.1.1 Major element concentrations on the surface of untreated MSWI fly ash particles. Samples were taken from gas cooling tower. Samples on the left side are without and samples on the right side are with lime injection. μ: average concentration in weight percent. Rsd: relative standard deviation.

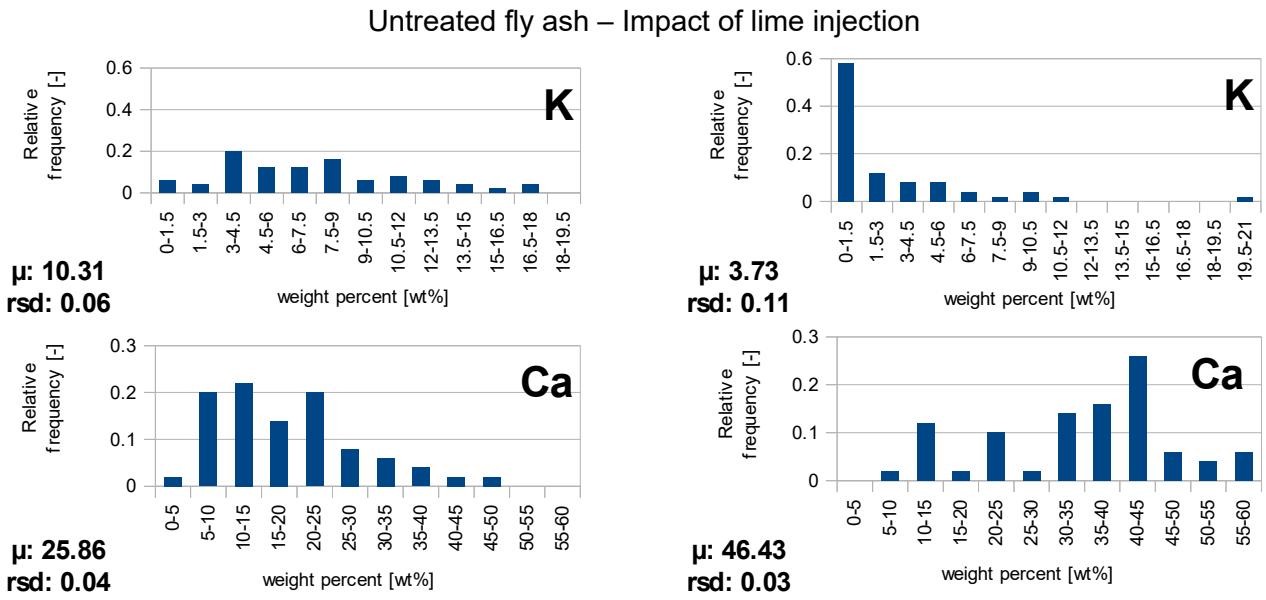

Figure 3.1.2 Major element concentrations on the surface of untreated MSWI fly ash particles. Samples were taken from gas cooling tower. Samples on the left side are without and samples on the right side are with lime injection. μ: average concentration in weight percent. Rsd: relative standard deviation.

Impact of gas temperature at lime injection

By comparing the results shown in figure 3.1.3 and 3.1.4 the impact of a changed injection point with different flue gas temperatures on particle surface heterogeneity is rather low. Only aluminium and silicon are slightly more homogeneous distributed. All other observed elements show almost the same values. Regarding weight percentage chlorine increases and calcium decreases when lime is injected at point 2. Maybe the neutralization reaction between Calcium hydroxide and hydrogen chloride is shifted more towards completion. Therefore less species of calcium hydroxide chloride CaOHCl, but more calcium chloride $CaCl_2$ is formed, which has been described by F. Bodénan et al. [5].

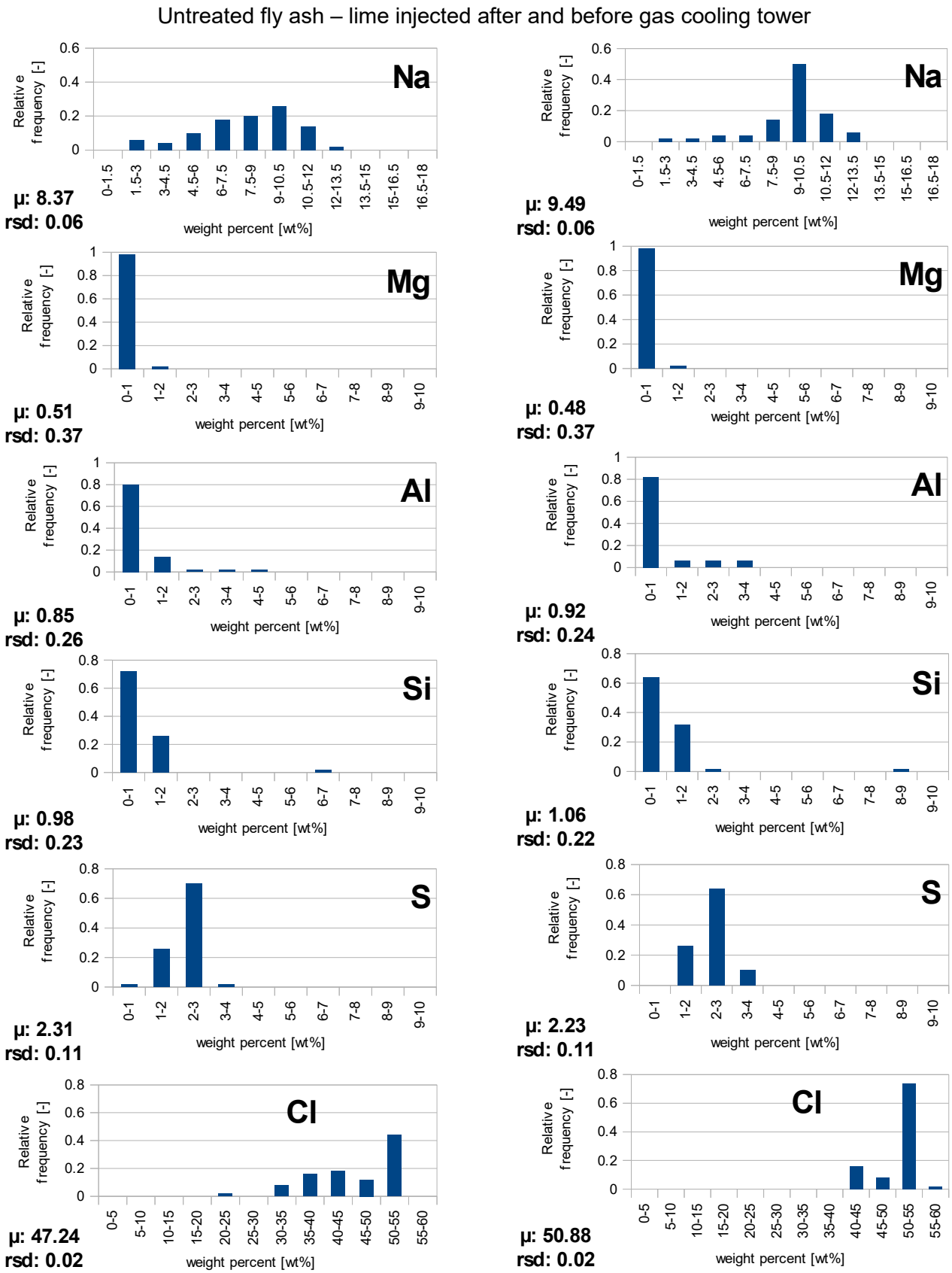

Figure 3.1.3 Major element concentrations on the surface of untreated MSWI fly ash particles derived from filter-type dust collector. Lime injection was carried out after for left samples and before gas cooling tower for right samples. μ: average concentration in weight percent. Rsd: relative standard deviation.

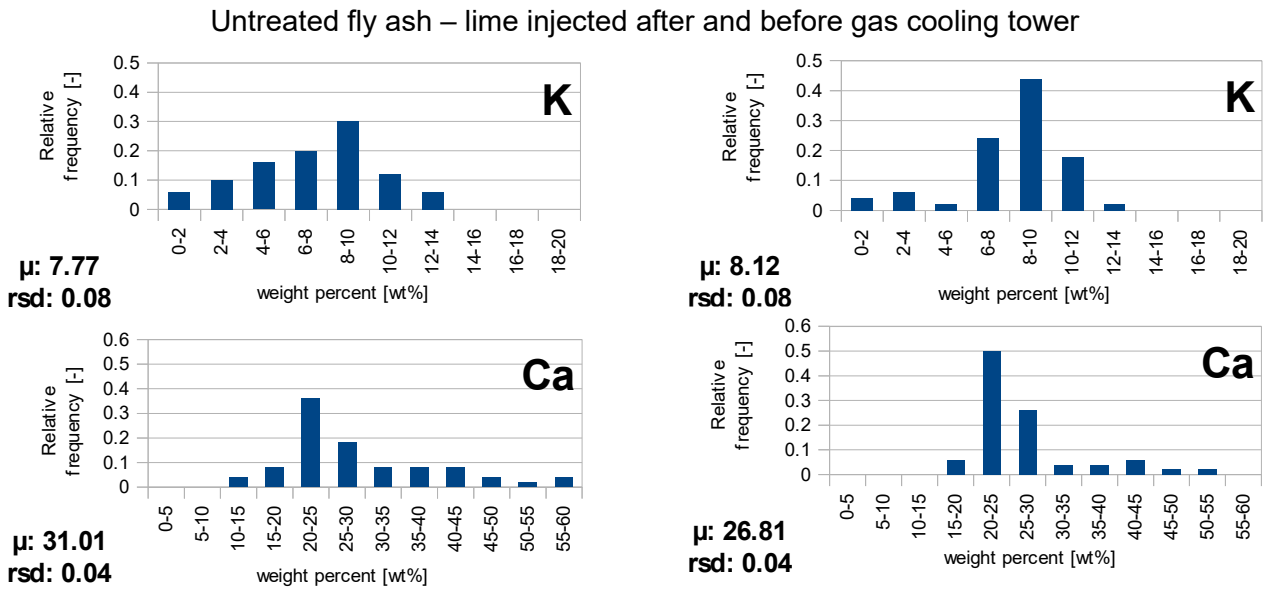

Figure 3.1.4 Major element concentrations on the surface of untreated MSWI fly ash particles derived from filter-type dust collector. Lime injection was carried out after for left samples and before gas cooling tower for right samples. μ: average concentration in weight percent. Rsd: relative standard deviation.

II) Japanese Leaching Test 46 – wet treated fly ash

Impact of lime

Lime injection leads to lower average weight percentages for all elements except calcium, chlorine and sulphur which are either injected into and absorbed from flue gas stream. Inter-particle heterogeneity increases when lime is used, only calcium, chlorine and sulphur become more homogeneous. Results are shown in figure 3.1.6 and 3.1.7.

Secondary mineral formation on the particle surface was not significant. The reason may be the shaking while performing JLT46. In contrast Hiroki Kitamura et. al. performed wet treatment on fly ash particles without shaking and they found massive secondary mineral formation. SEM-fotos are shown in figure 3.1.5 where untreated fly ash samples are compared to wet-treated ones.

Untreated fly ash JLT46 wet-treated fly ash

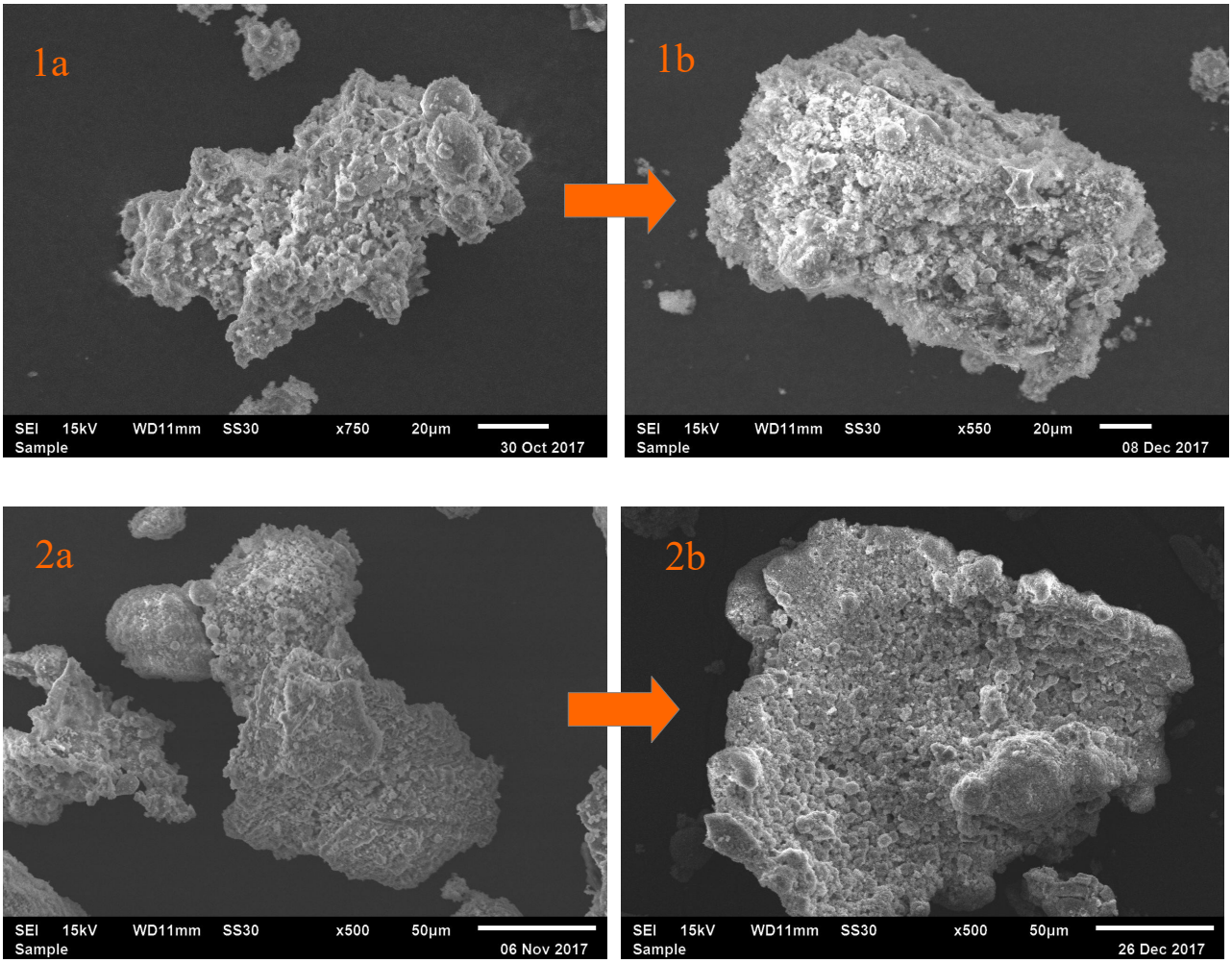

Figure 3.1.5 Comparison of untreated fly ash samples with wet-treated fly ash samples. a) untreated fly ash sample; b) JLT46 wet-treated fly ash sample; 1) sample taken from gas cooling tower with no lime injection; 2) sample taken from gas cooling tower with lime injection before gas cooling tower

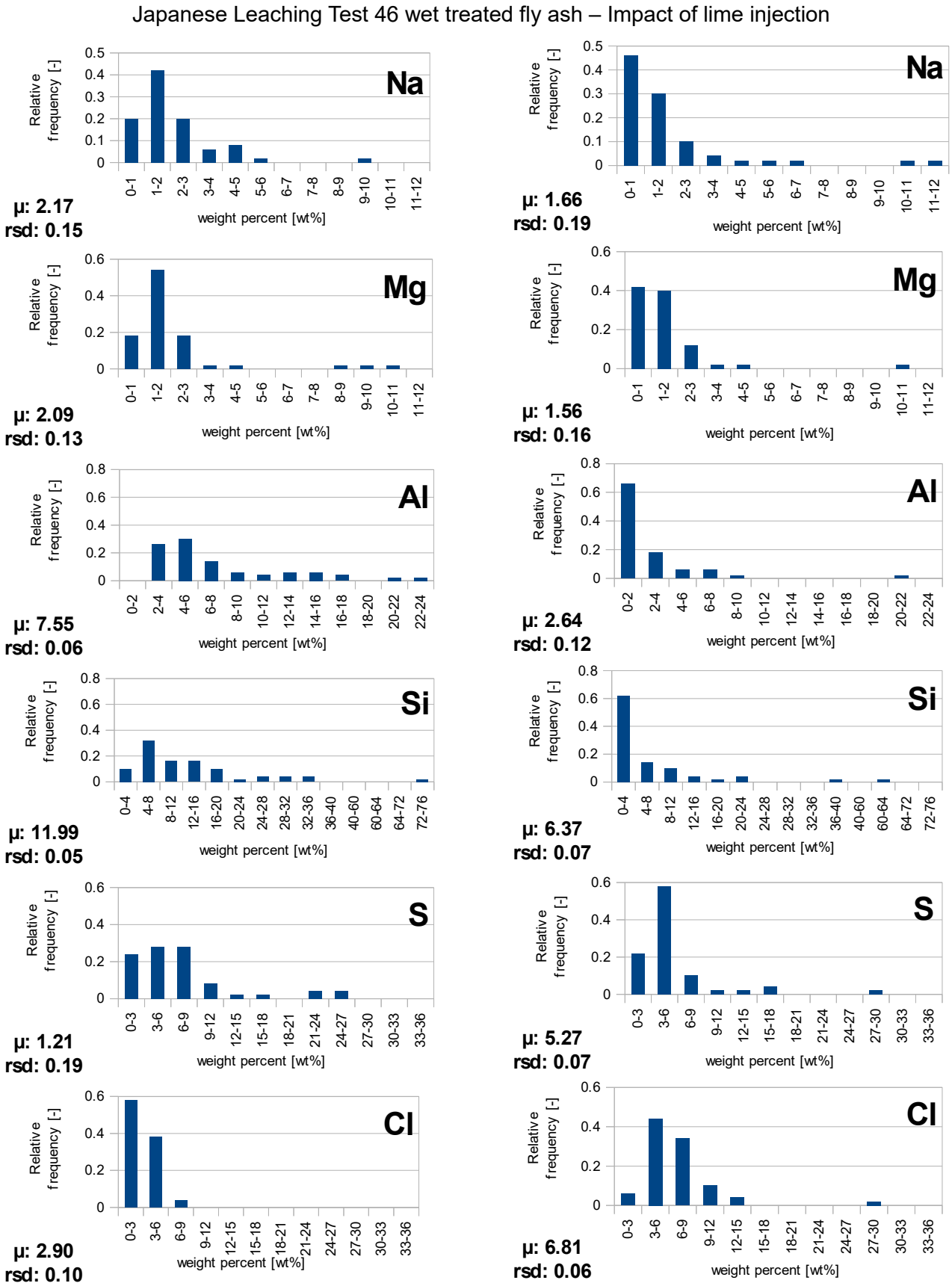

Figure 3.1.6 Major element concentrations on the surface of MSWI fly ash particles after JLT46. Samples were taken from gas cooling tower. Samples on the left side are without and samples on the right side are with lime injection. μ: average concentration in weight percent. Rsd: relative standard deviation.

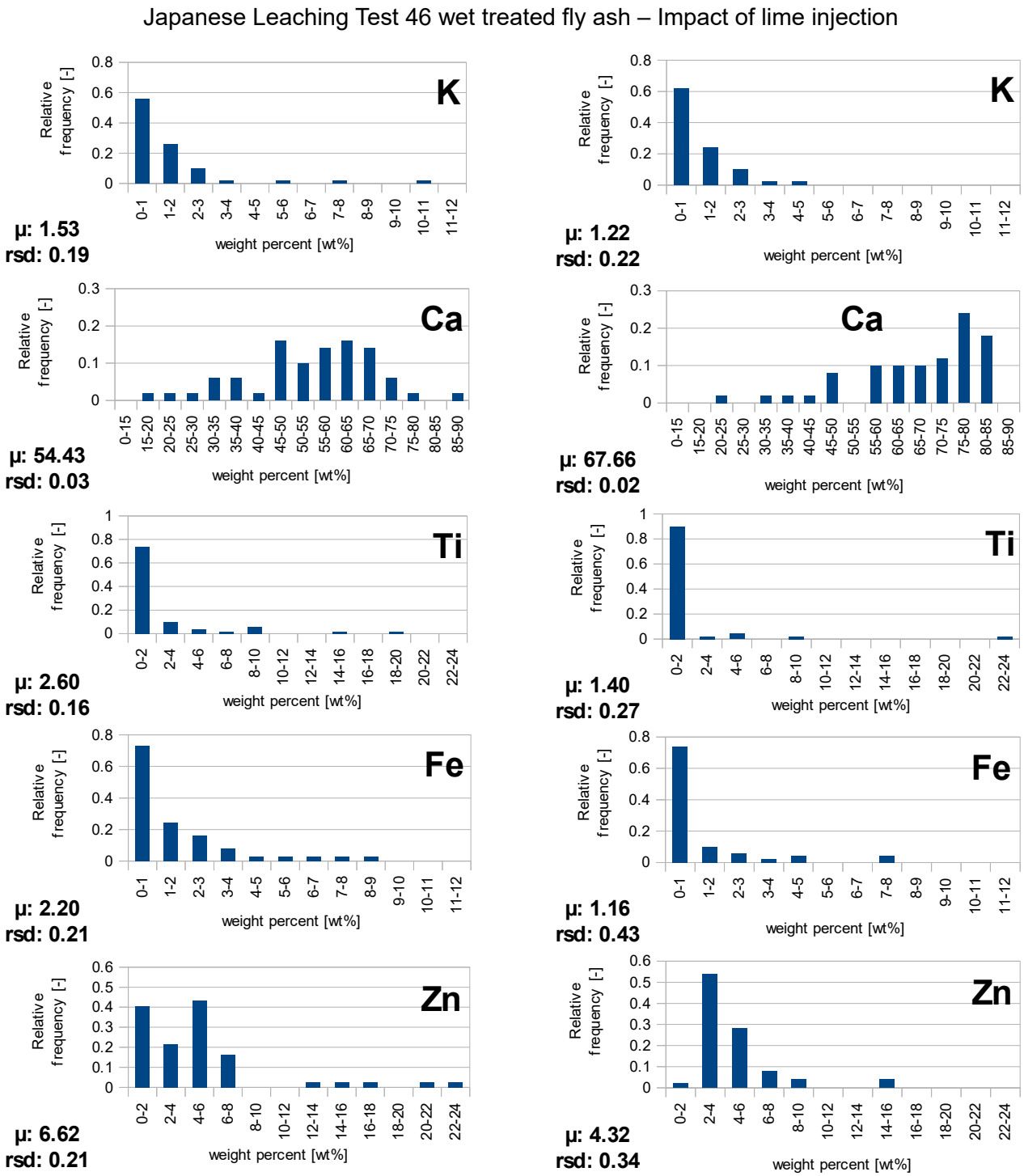

Figure 3.1.7 Major element concentrations on the surface of MSWI fly ash particles after JLT46. Samples were taken from gas cooling tower. Samples on the left side are without and samples on the right side are with lime injection. μ: average concentration in weight percent. Rsd: relative standard deviation.

Impact of gas temperature at lime injection

The difference between the two lime injection points on the particle surface heterogeneity is rather low. As for the untreated fly ash chlorine content increases and calcium content decreases when lime slurry is added before gas cooling tower (point 2). Regarding inter-particle heterogeneity sodium and zinc are more homogeneous while titan is more heterogeneous distributed on fly ash particle surfaces when calcium hydroxide slurry is injected earlier (= injection point 2) in the process. All results are shown in figure 3.1.9 and 3.1.10.

Secondary mineral formation was not observable. In figure 3.1.8 fotos are shown exemplarily.

Untreated fly ash JLT46 wet-treated fly ash

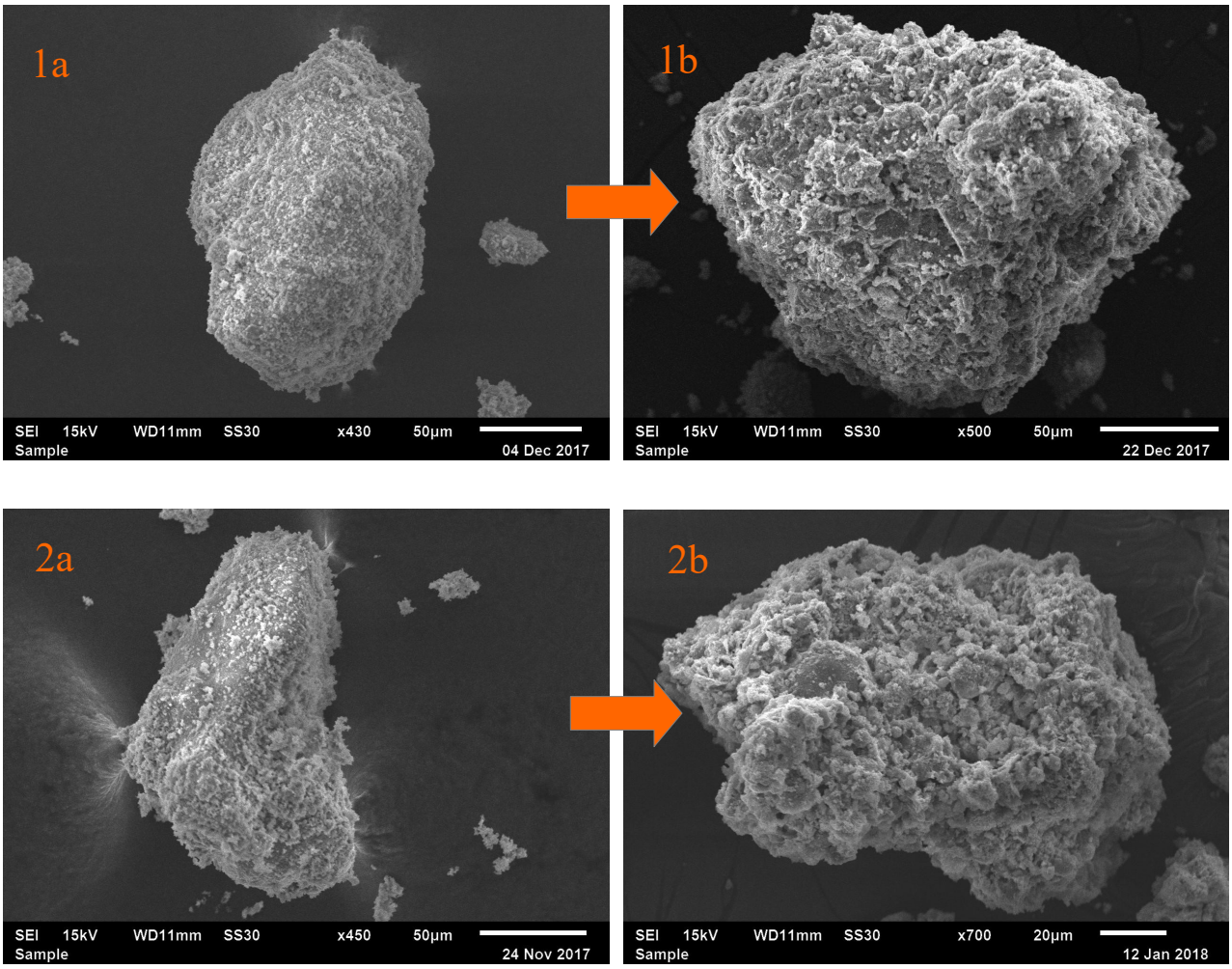

Figure 3.1.8 Comparison of untreated fly ash samples with wet-treated fly ash samples. a) untreated fly ash sample; b) JLT46 wet-treated fly ash sample; 1) sample taken from filter-type dust collector with lime injection after gas cooling tower; 2) sample taken from filter-type dust collector with lime injection before gas cooling tower

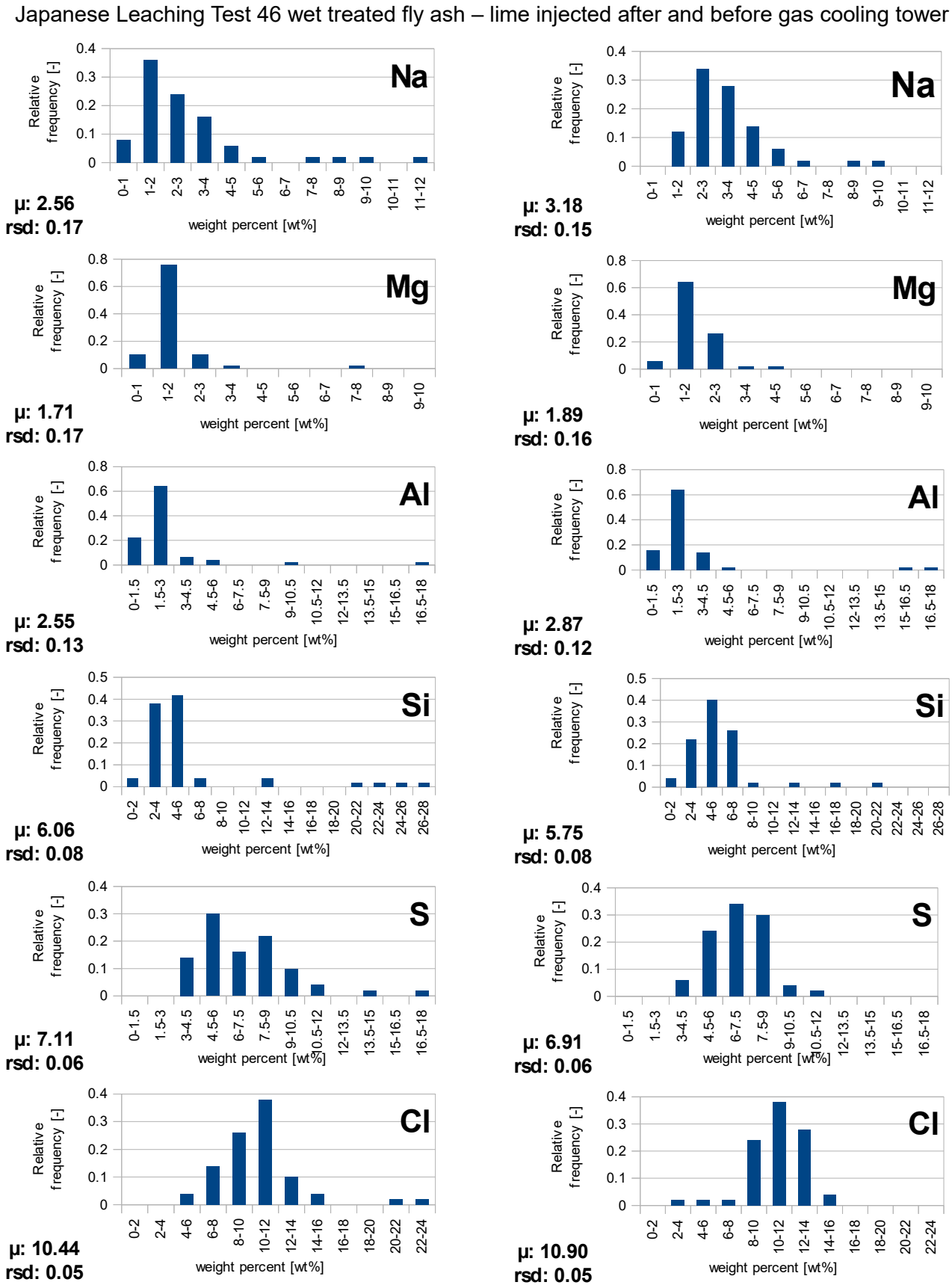

Figure 3.1.9 Major element concentrations on the surface of untreated MSWI fly ash particles derived from filter-type dust collector after JLT46. Lime injection was carried out after for left samples and before gas cooling tower for right samples. μ: average concentration in weight percent. Rsd: relative standard deviation.

Japanese Leaching Test 46 wet treated fly ash – lime injected after and before gas cooling tower

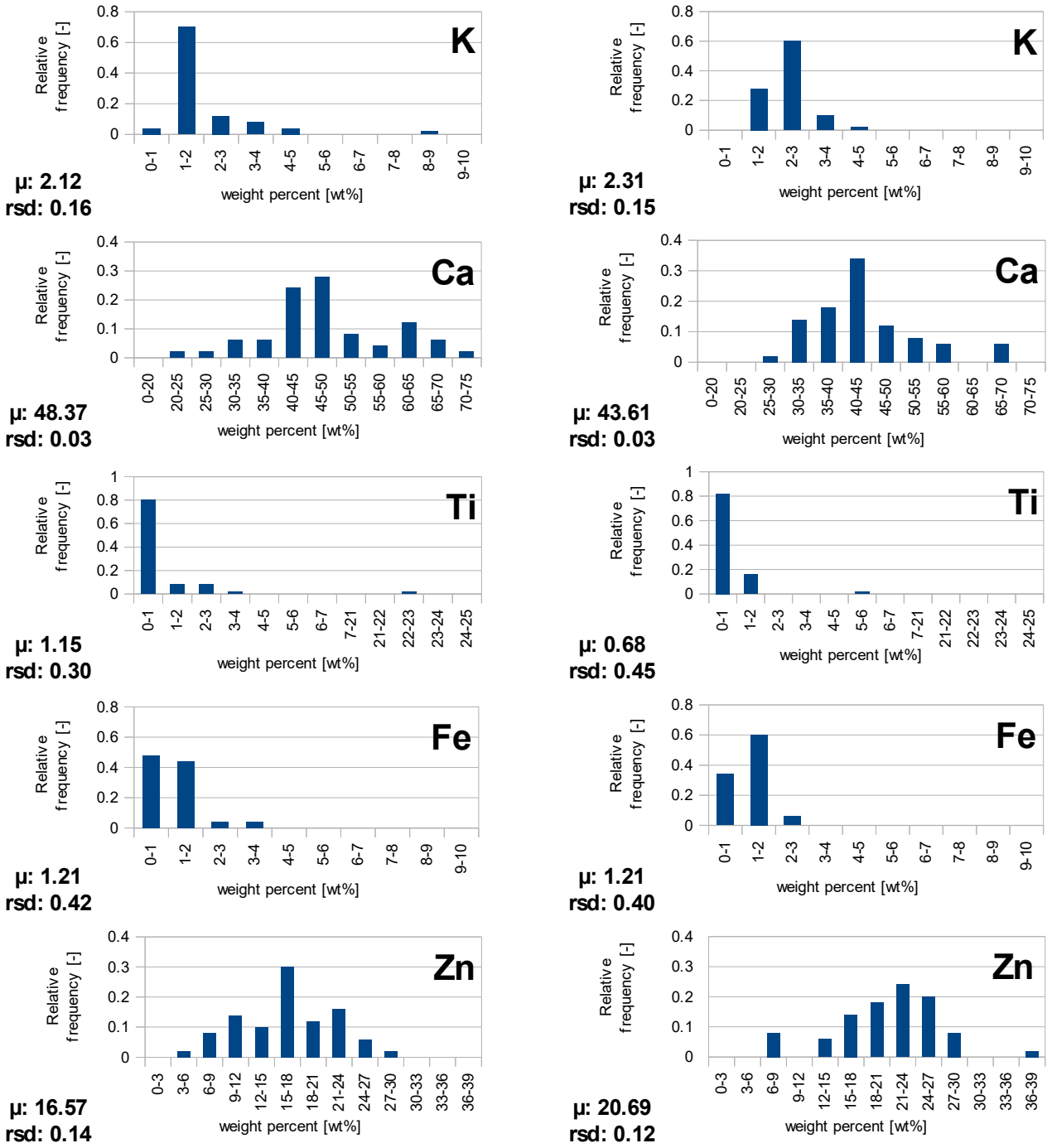

Figure 3.1.10 Major element concentrations on the surface of untreated MSWI fly ash particles derived from filter-type dust collector after JLT46. Lime injection was carried out after for left samples and before gas cooling tower for right samples. μ: average concentration in weight percent. Rsd: relative standard deviation.

III) Toxicity Characteristic Leaching Procedure – mid-part of fly ash particles

Impact of lime

The injection of calcium hydroxide slurry triggers higher inter-particle heterogeneity of the mid-part of fly ash particles for many elements as shown in figure 3.1.11 and 3.1.12. Inter-particle heterogeneity of magnesium and silicon remain unrevised. Sulphur and chlorine absorption seems to increase with lime injection and therefore their distribution gets more homogeneous at the mid-part of fly ash particles. It should be noted that calcium is still the major element with ~60wt% followed by sulphur with ~10wt%. Chlorine species should be dissolved and therefore the chlorine content amounts to only 2.3wt%. Further should be noted that the distribution of calcium becomes also more homogeneous if compared to not neutralized fly ash samples.

Impact of gas temperature at lime injection

In figure 3.1.13 and 3.1.14 there is the according mid-part analysis shown. By comparing the results it seems the inter-particle homogeneity of sodium, potassium and the observed transition metals increases when lime is injected at point 2. On the other hand the distribution of the remaining elements does not change that much. It should be noted that the zinc content of both samples is rather high with more than 20wt%.

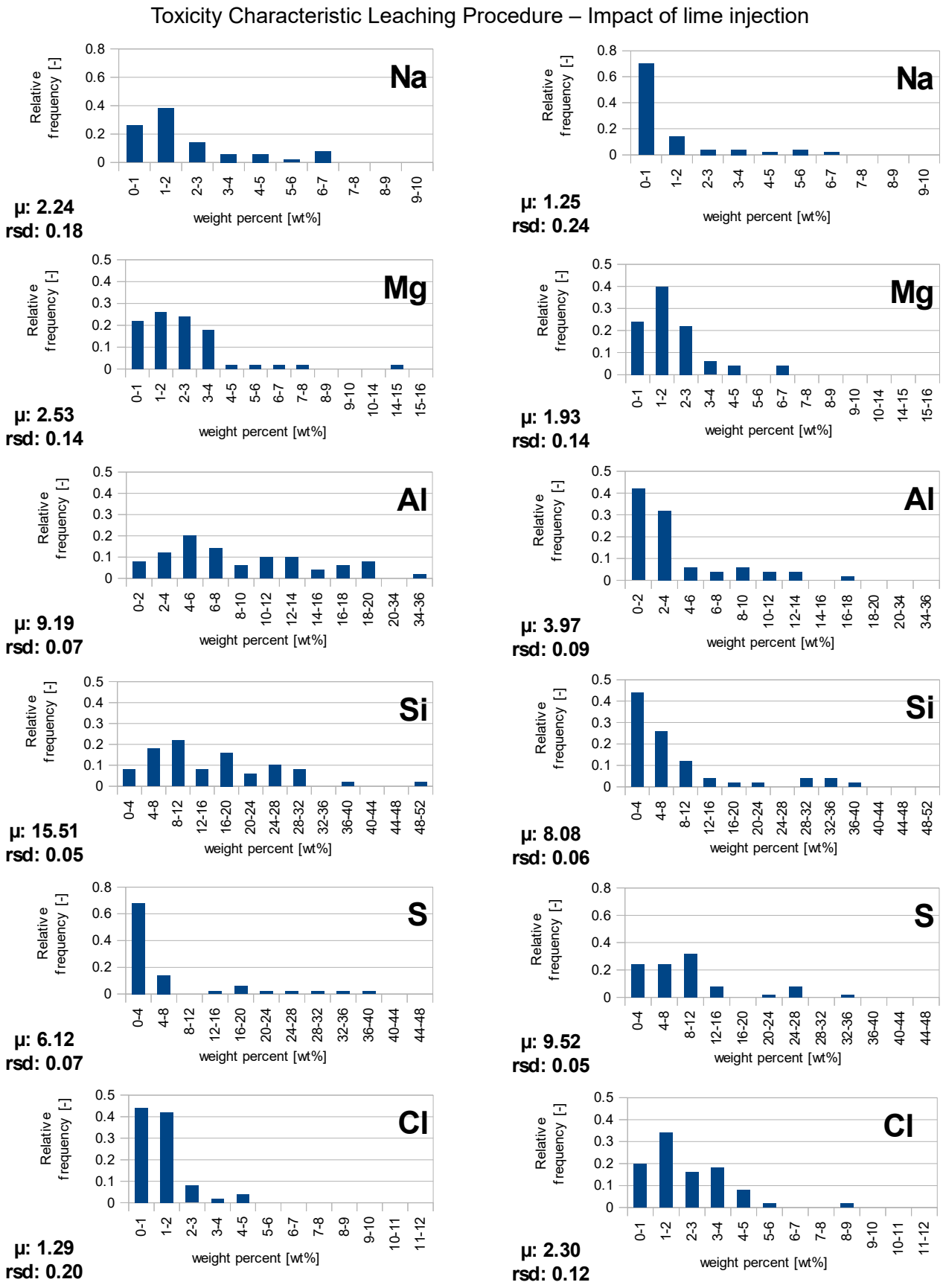

Figure 3.1.11 Major element concentrations of MSWI fly ash particles after TCLP. Samples were taken from gas cooling tower. Samples on the left side are without and samples on the right side are with lime injection. μ: average concentration in weight percent. Rsd: relative standard deviation.

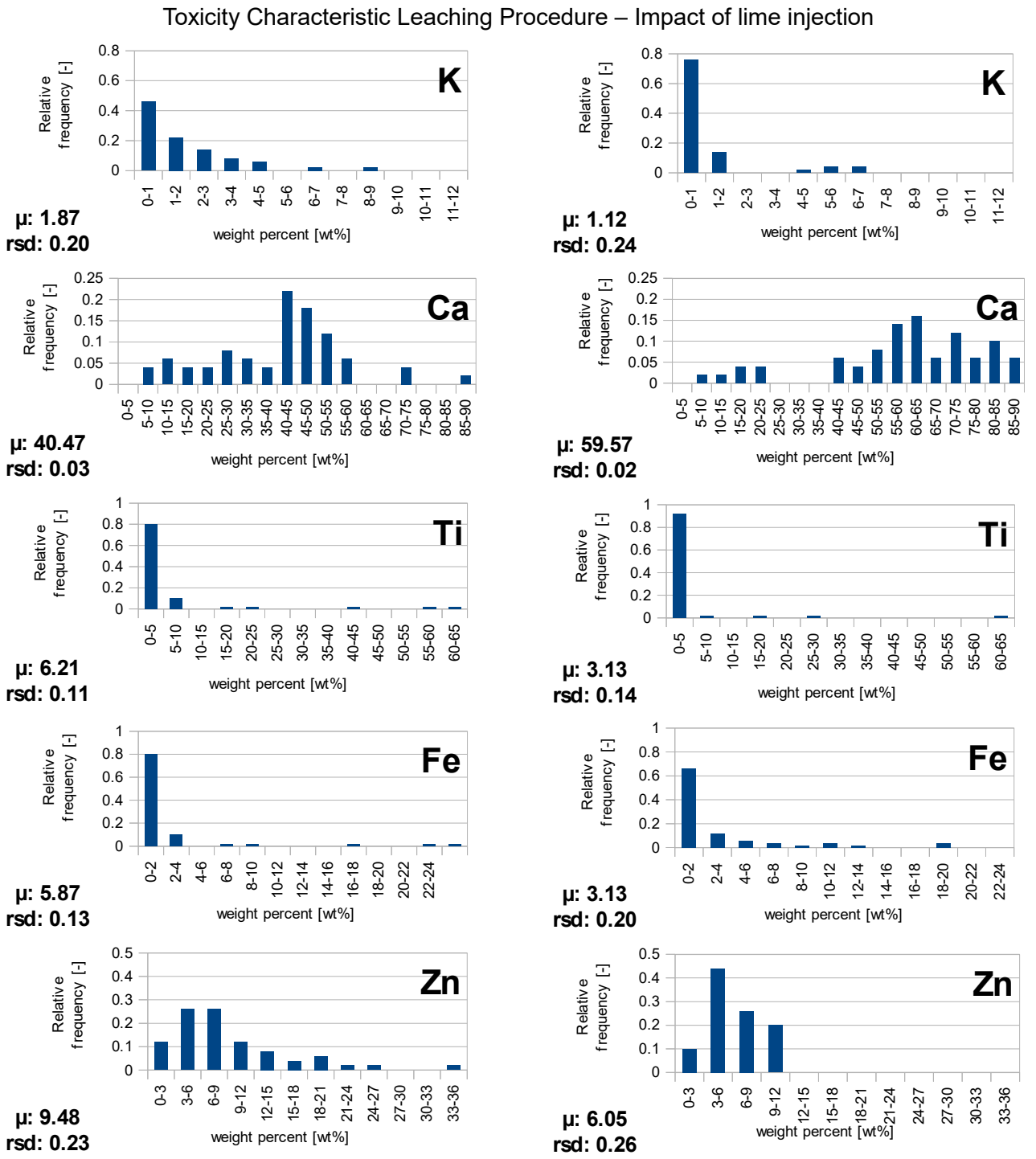

Figure 3.1.12 Major element concentrations of MSWI fly ash particles after TCLP. Samples were taken from gas cooling tower. Samples on the left side are without and samples on the right side are with lime injection. μ: average concentration in weight percent. Rsd: relative standard deviation.

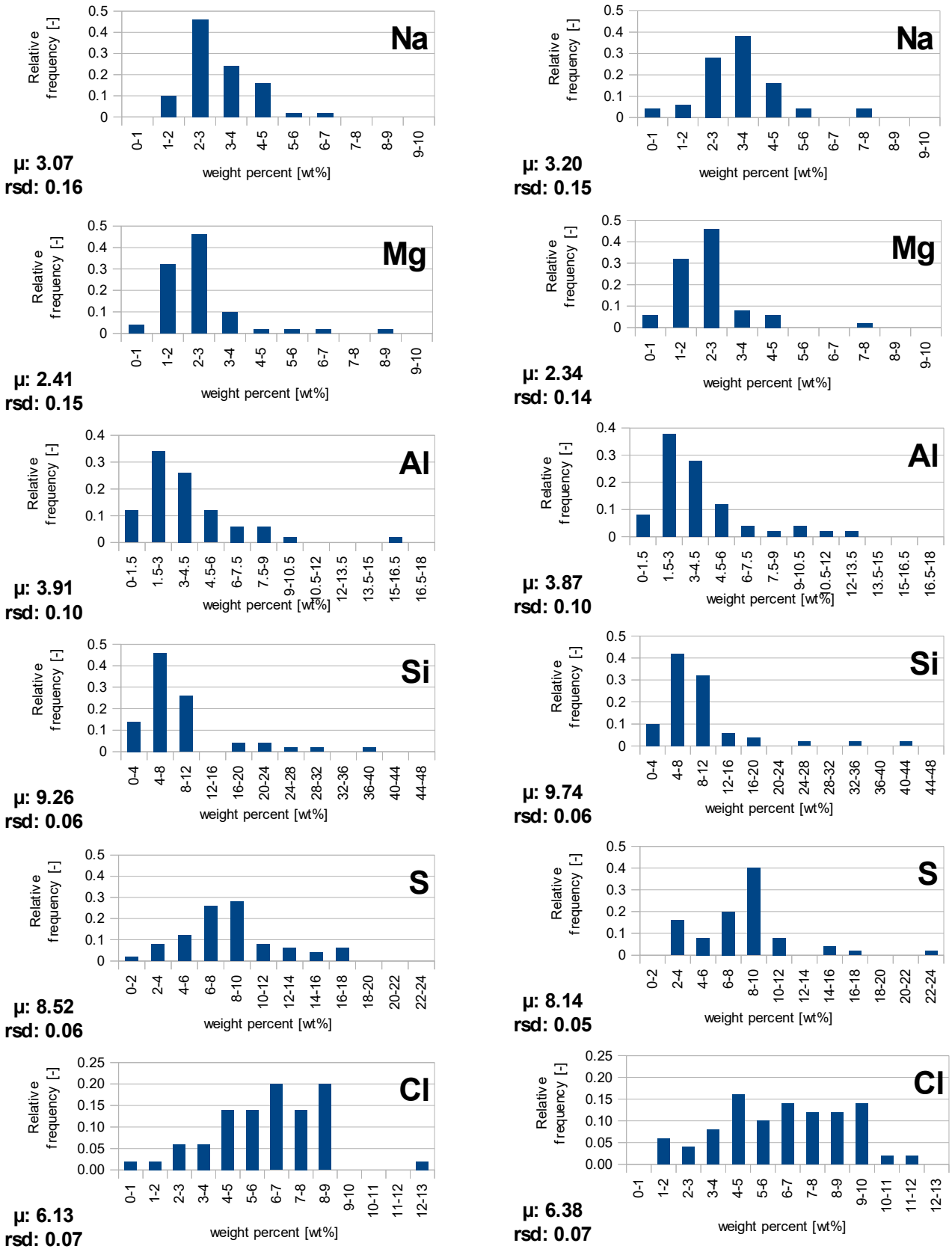

Figure 3.1.13 Major element concentrations on the surface of MSWI fly ash particles after TCLP. Samples were taken from filter-type dust collector. Lime injection was carried out after for left samples and before gas cooling tower for right samples. μ: average concentration in weight percent. Rsd: relative standard deviation.

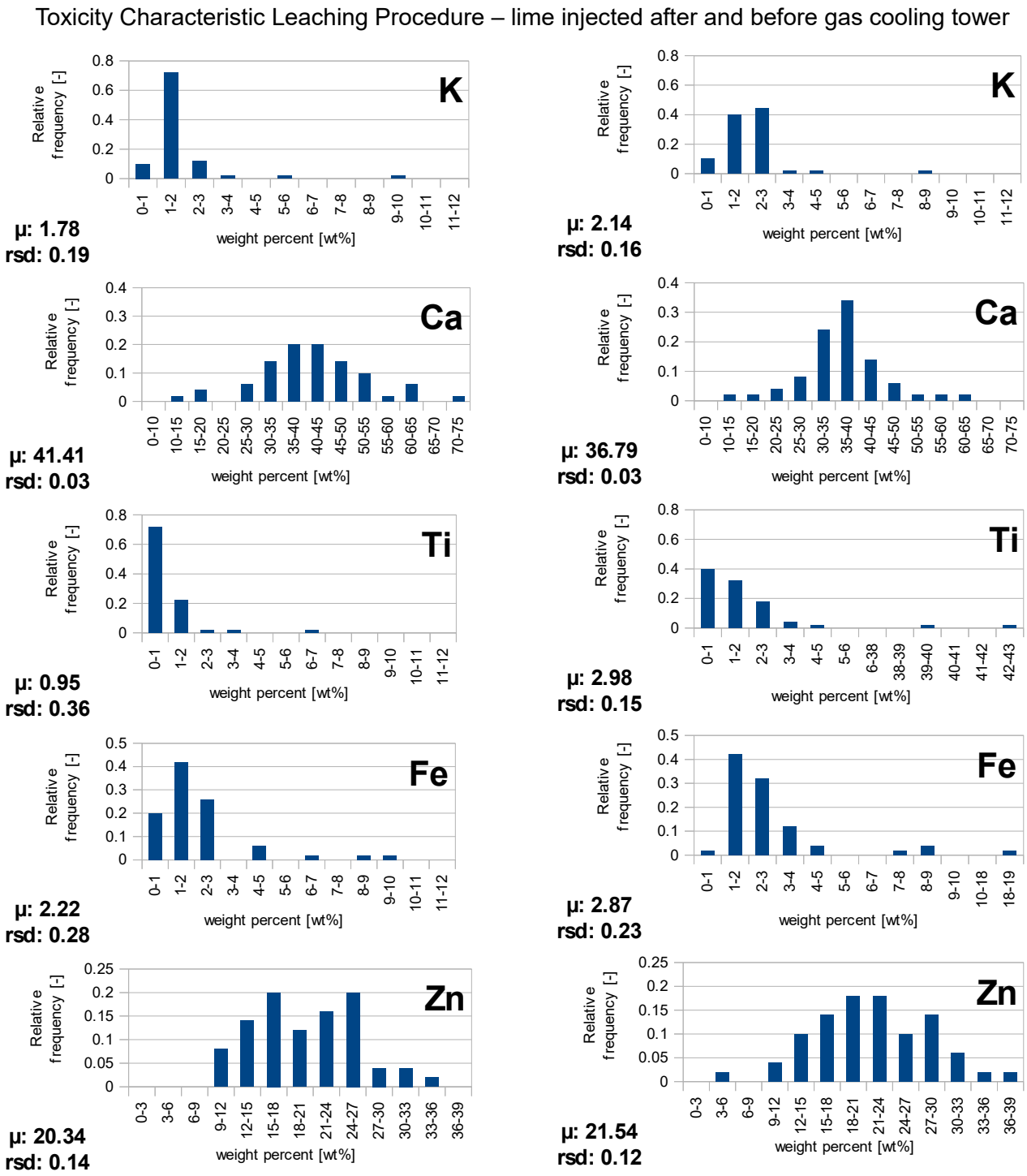

Figure 3.1.14 Major element concentrations on the surface of MSWI fly ash particles after TCLP. Samples were taken from filter-type dust collector. Lime injection was carried out after for left samples and before gas cooling tower for right samples. μ: average concentration in weight percent. Rsd: relative standard deviation.

IV) Japanese Leaching Test 19 – core of fly ash particles

Impact of lime

The investigation of the fly ash particle core after Japanese Leaching Test 19 leads to the assumption that calcium hydroxide addition has a small impact on inter-particle heterogeneity. Most observed elements show same distributions that is why the difference of calculated values are in a margin of 0.01 as shown in figure 3.1.15 and 3.1.16. Sulphur and potassium show a more homogeneous and titan and zinc a more heterogeneous inter-particle distribution regarding particle core when limestone is injected.

Impact of gas temperature at lime injection

It seems like injected lime at point 2 leads to more inter-particle homogeneity of fly ash particle cores. This holds true for all elements even those with small differences like silicon and chlorine. Furthermore that means the greatest impact of the second lime injection point on inter-particle heterogeneity. On the mid-part and surface of fly ash particles the effect was rather low in comparison. All relevant data is shown in figure 3.1.17 and 3.1.18.

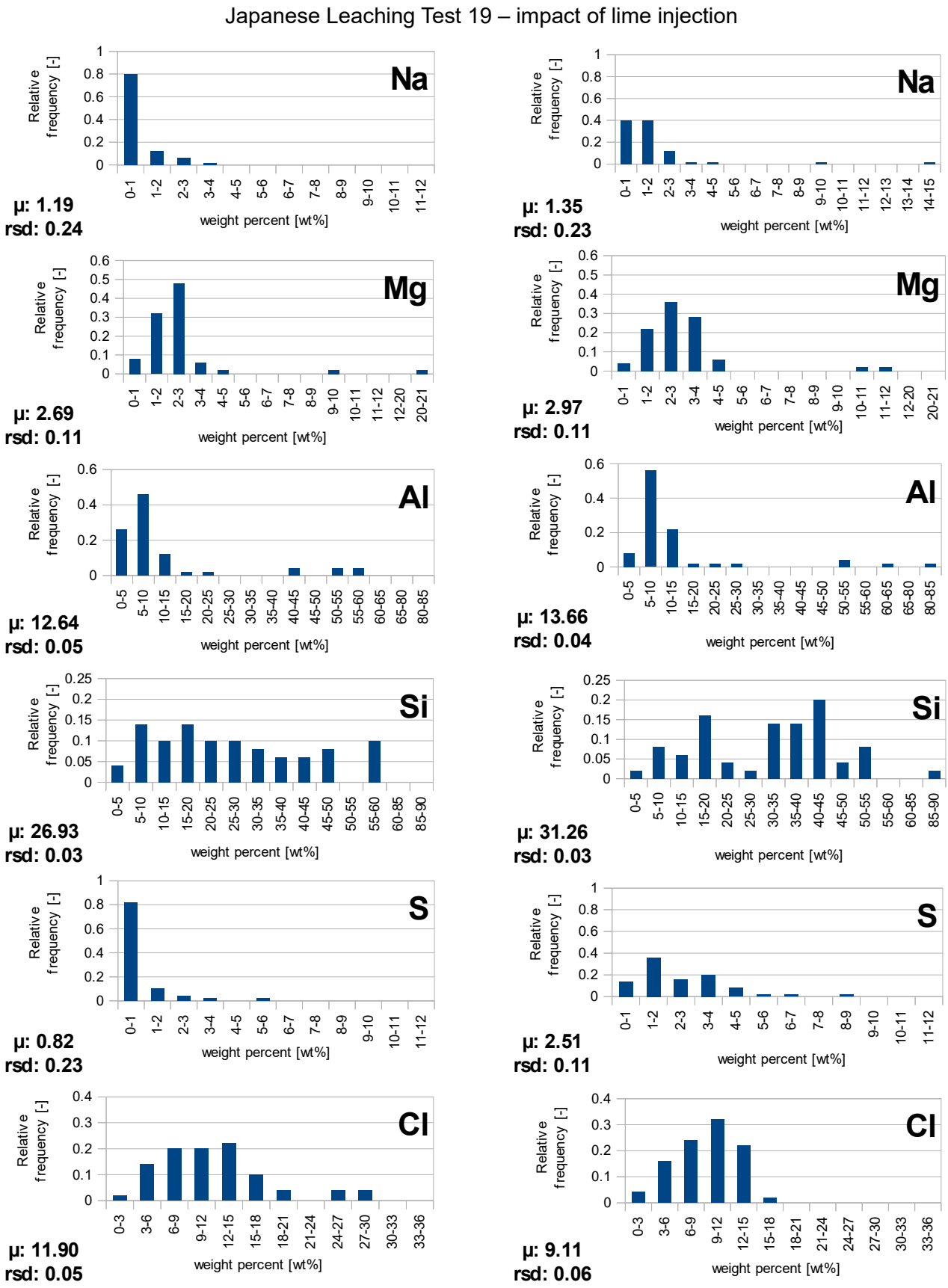

Figure 3.1.15 Major element concentrations of MSWI fly ash particles after JLT19. Samples were taken from gas cooling tower. Samples on the left side are without and samples on the right side are with lime injection. μ: average concentration in weight percent. Rsd: relative standard deviation.

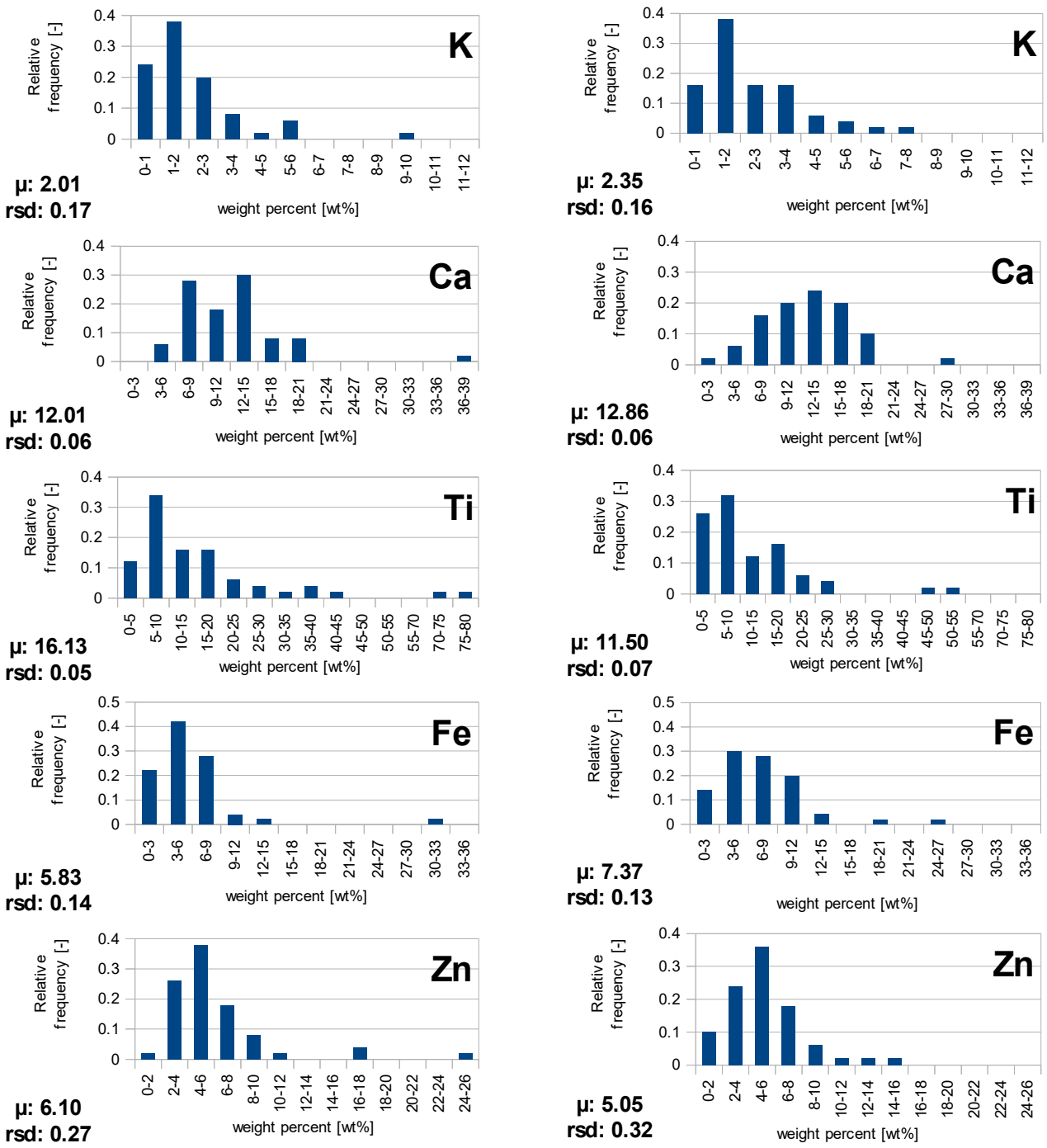

Figure 3.1.16 Major element concentrations of MSWI fly ash particles after JLT19. Samples were taken from gas cooling tower. Samples on the left side are without and samples on the right side are with lime injection. μ: average concentration in weight percent. Rsd: relative standard deviation.

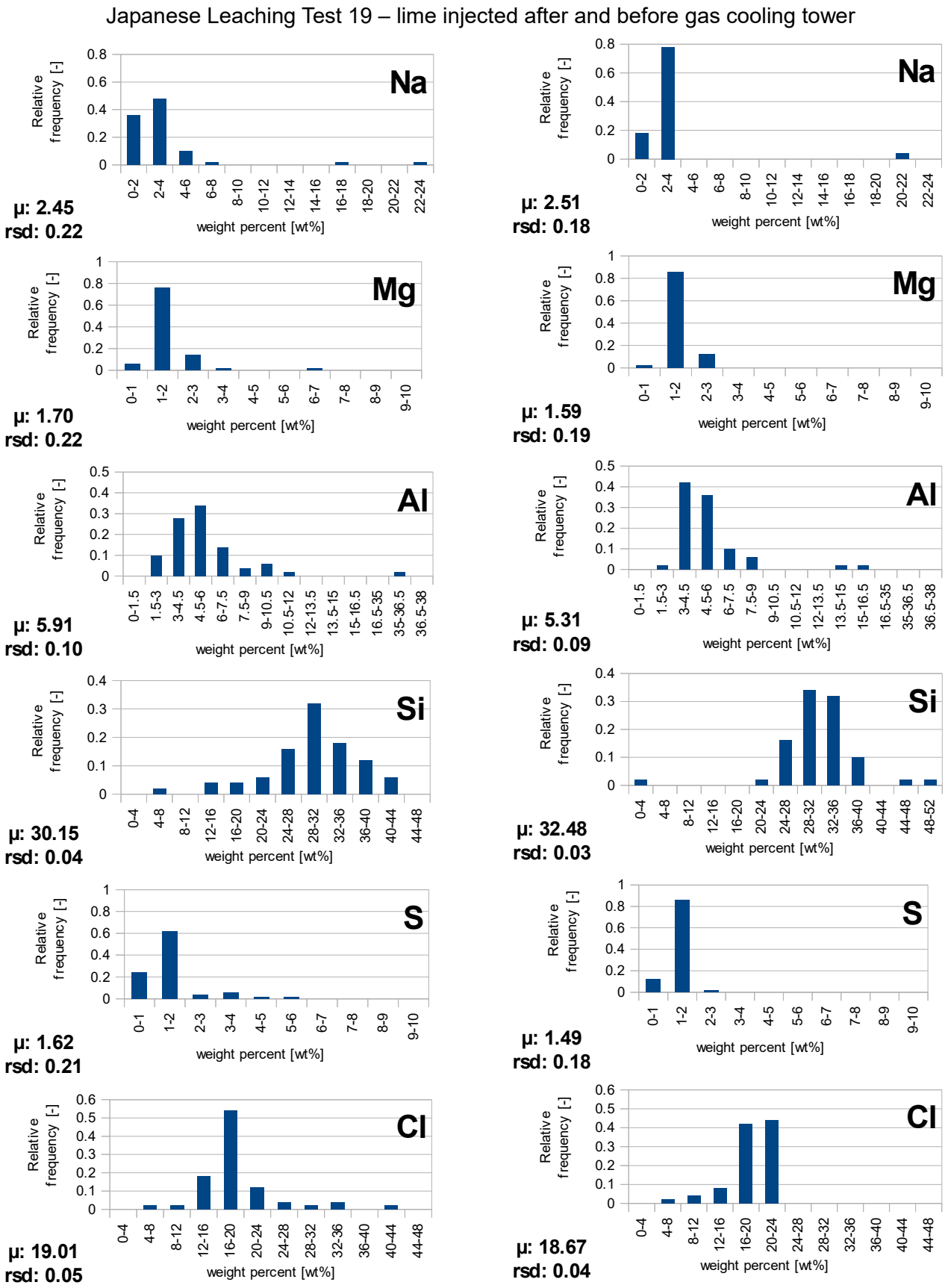

Figure 3.1.17 Major element concentrations on the surface of MSWI fly ash particles after JLT19. Samples were taken from filter-type dust collector. Lime injection was carried out after for left samples and before gas cooling tower for right samples. μ: average concentration in weight percent. Rsd: relative standard deviation.

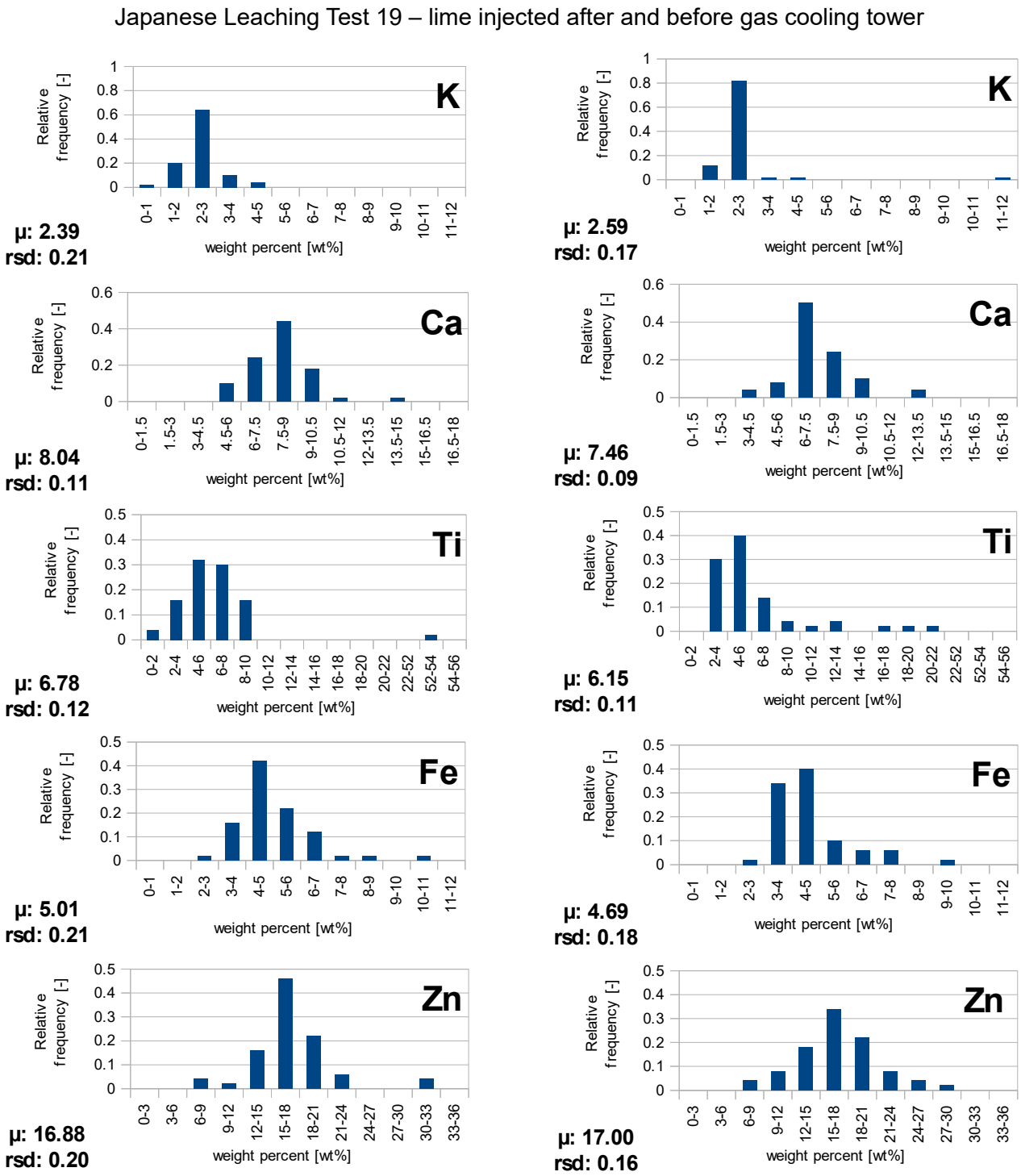

Figure 3.1.18 Major element concentrations on the surface of MSWI fly ash particles after JLT19. Samples were taken from filter-type dust collector. Lime injection was carried out after for left samples and before gas cooling tower for right samples. μ: average concentration in weight percent. Rsd: relative standard deviation.

3.2. *Intra-particle Heterogeneity*

I) Untreated fly ash samples

Impact of lime injection

The data shown in figure 3.2.1 and 3.2.2 show both samples taken from the gas cooling unit and it leads to the rather clear assumption that injected calcium hydroxide triggers intra-particle homogeneity on the fly ash particle surface. All observed elements show lower coefficients of variation. The lowest difference can be observed for aluminium with 0.01 and the highest for potassium with a change of 0.11 of the coefficient of variation. Regarding many elements there are particles with high coefficients of variation. It seems there are hotspots with high concentration of that element which leads to higher CV values.

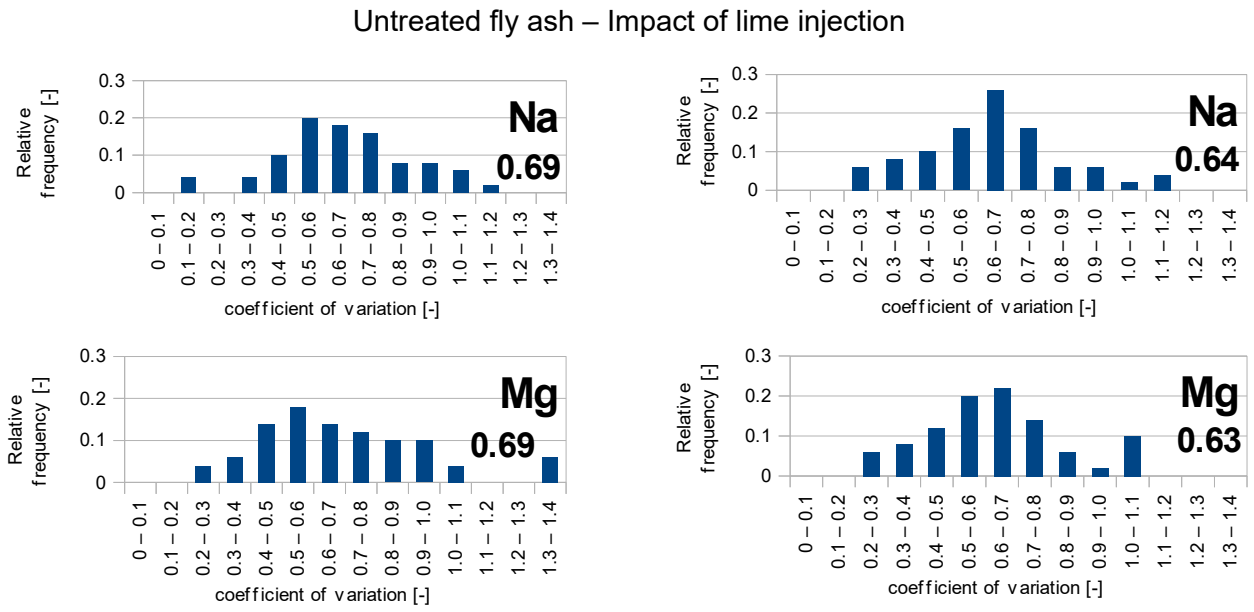

Figure 3.2.1 Coefficient of variation of major elements in untreated fly ash samples taken from gas cooling tower. Samples on the left side are without and samples on the right side are with lime injection. Values shown in each figure are average CV values of each element.

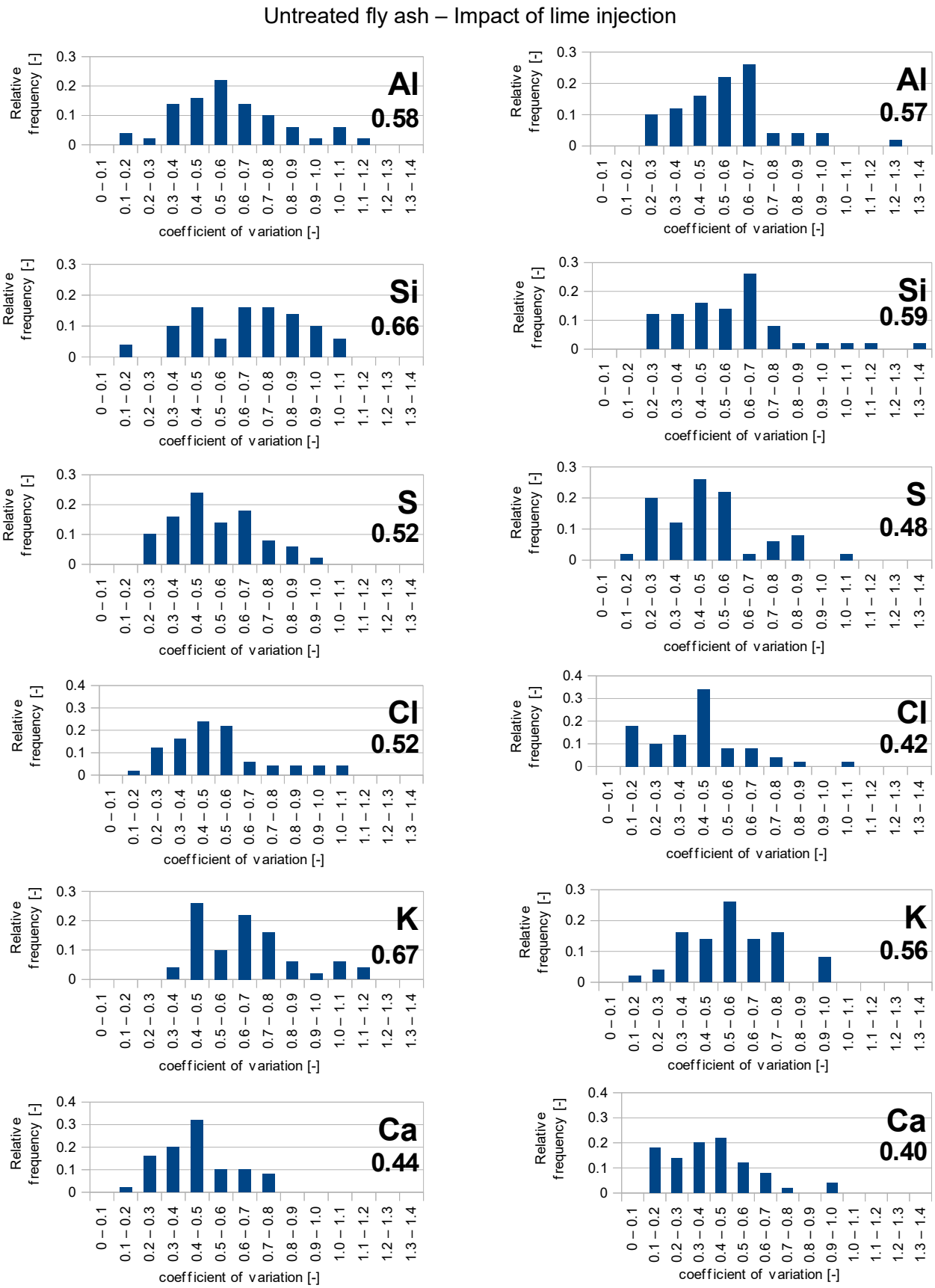

Figure 3.2.2 Coefficient of variation of major elements in untreated fly ash samples taken from gas cooling tower. Samples on the left side are without and samples on the right side are with lime injection. Values shown in each figure are average CV values of each element.

Impact of gas temperature at lime injection

Changing the injection point has a limited effect on intra-particle heterogeneity on fly ash particle surface. Most elements show a slightly increase in heterogeneity if calcium hydroxide is added at point 2 of the incineration plant as it can be seen in figure 3.2.3 and 3.2.4. Potassium is the only element which is distributed more homogeneous regarding intra-particle heterogeneity. Sodium does not change and gives in both cases the same coefficient of variation.

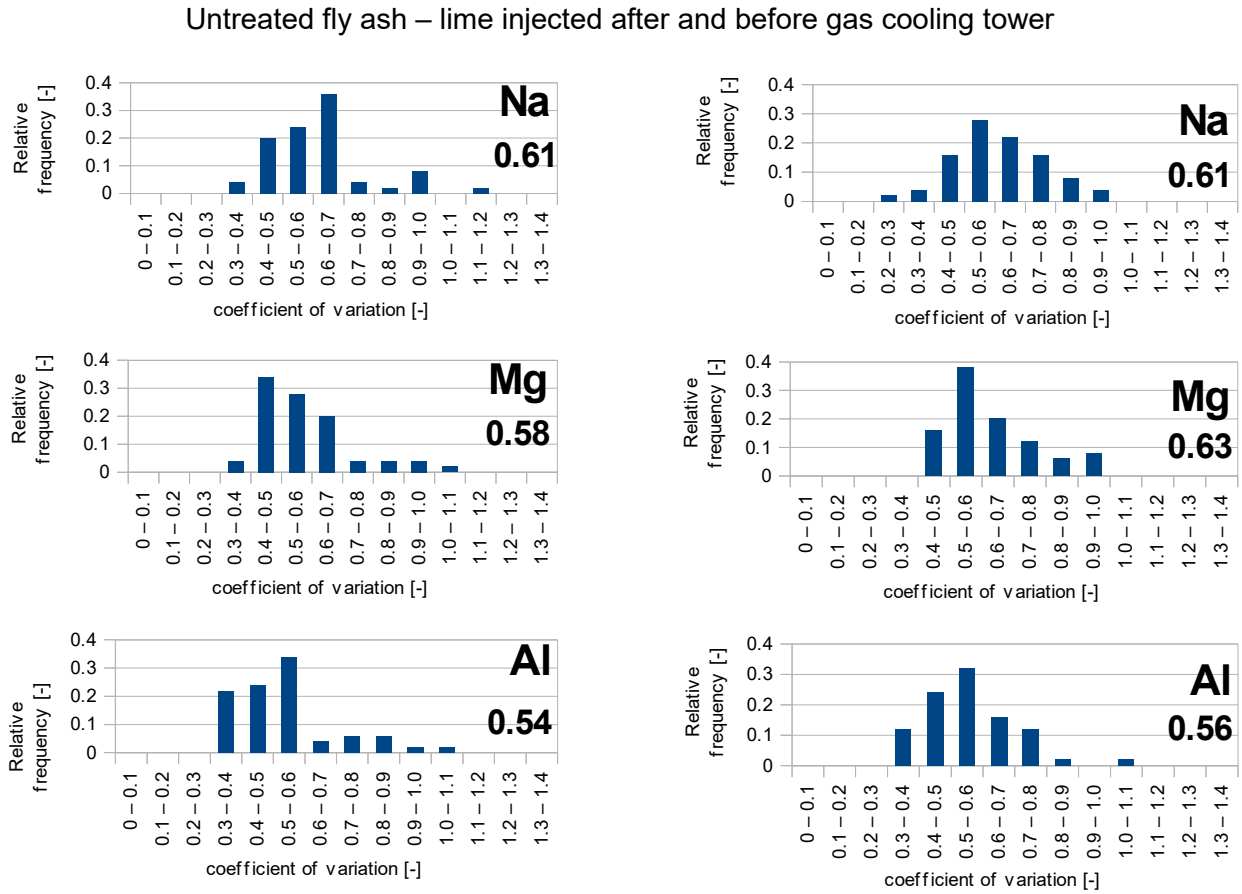

Figure 3.2.3 Major element concentrations on the surface of untreated MSWI fly ash particles derived from filter-type dust collector. Lime injection was carried out after for left samples and before gas cooling tower for right samples. Values shown in each figure are average CV values of each element.

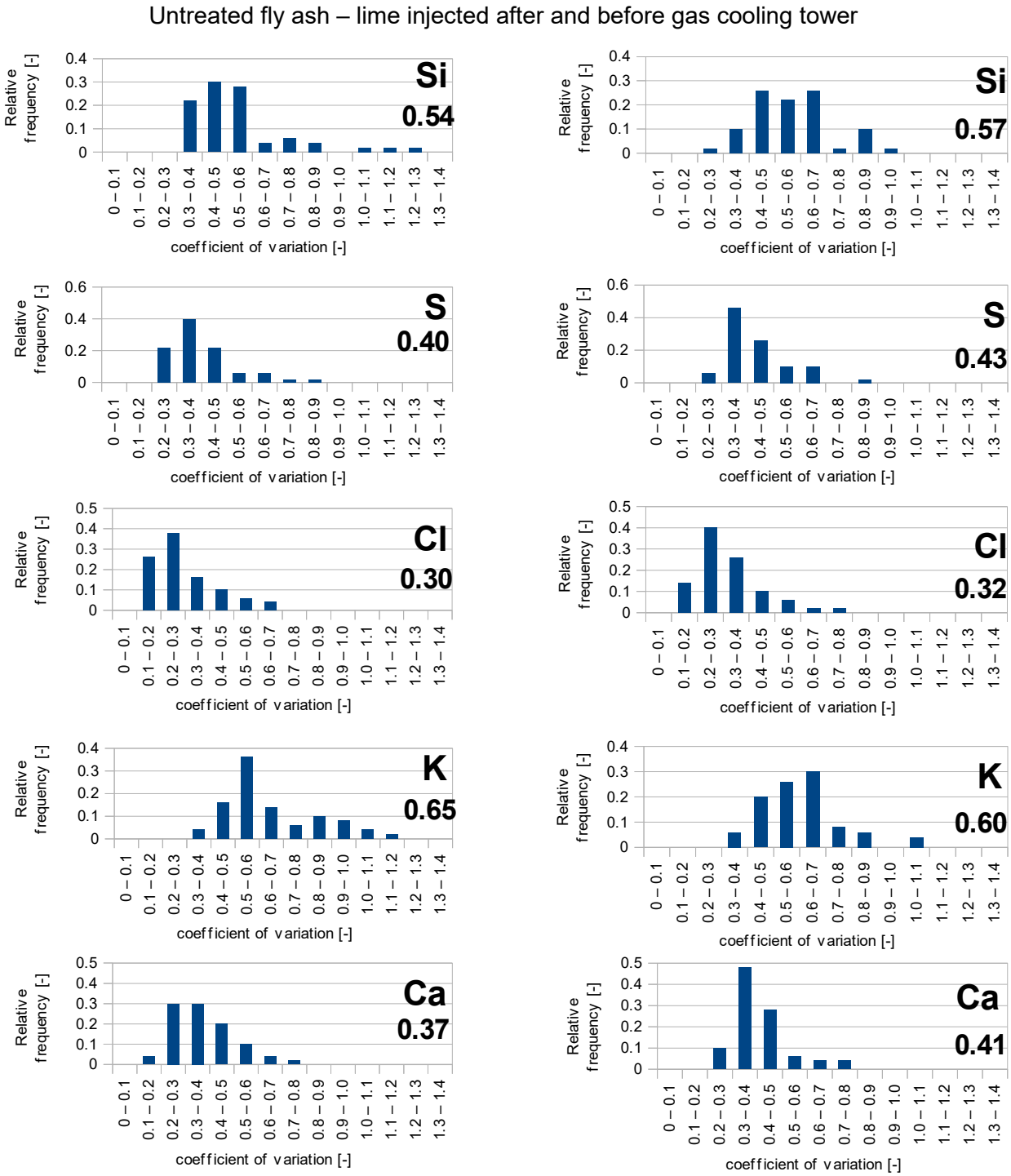

Figure 3.2.4 Major element concentrations on the surface of untreated MSWI fly ash particles derived from filter-type dust collector. Lime injection was carried out after for left samples and before gas cooling tower for right samples. Values shown in each figure are average CV values of each element.

II) Japanese Leaching Test 46 – wet treated fly ash

Impact of lime

With the addition of calcium hydroxide sodium, magnesium and chlorine become more heterogeneous regarding intra-particle heterogeneity. Among these elements sodium shows the hugest change in the average of the coefficient of variation with 0.17. On the other side magnesium does not change that much with just 0.01 as difference. Silicon and iron can be considered unchanged and all other elements increase their intra-particle homogeneity when lime is injected as it can be seen in figure 3.2.5 and 3.2.6.

Secondary mineral formation did not occur to that extend where it could be determined with SEM and the naked eye. Photos are shown in the section above *3.1.II) Japanese Leaching Test 46 wet-treated fly ash* in figure 3.1.5 on page 26.

Impact of gas temperature at lime injection

The wet treated fly ash sample from point 2 shows a more homogeneous intra-particle distribution on the particle surface. Only exceptions are aluminium which remains same for both samples and iron that becomes just slightly more heterogeneous. The elemental distributions are typically narrower and show a higher relative frequency as maximum if the sample becomes more homogeneous. As it can be seen in figure 3.2.7 and 3.2.8 where the data is shown.

Secondary mineral formation was also not observable. Photos are shown under point *3.1.II) Japanese Leaching Test 46 wet-treated fly ash* in figure 3.1.5 on page 26.

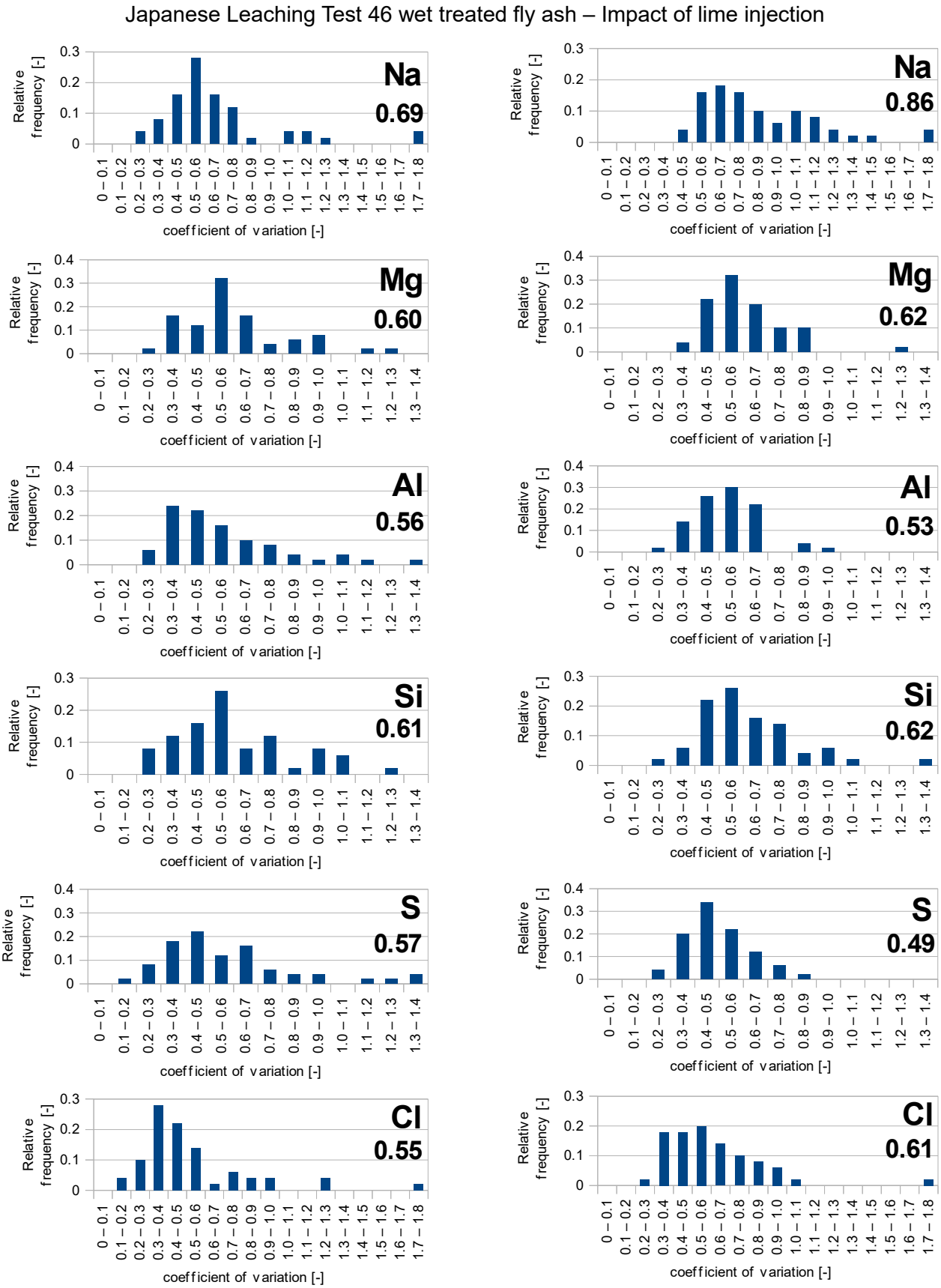

Figure 3.2.5 Major element concentrations on the surface of MSWI fly ash particles after JLT46. Samples were taken from gas cooling tower. Samples on the left side are without and samples on the right side are with lime injection. Values shown in each figure are average CV values of each element.

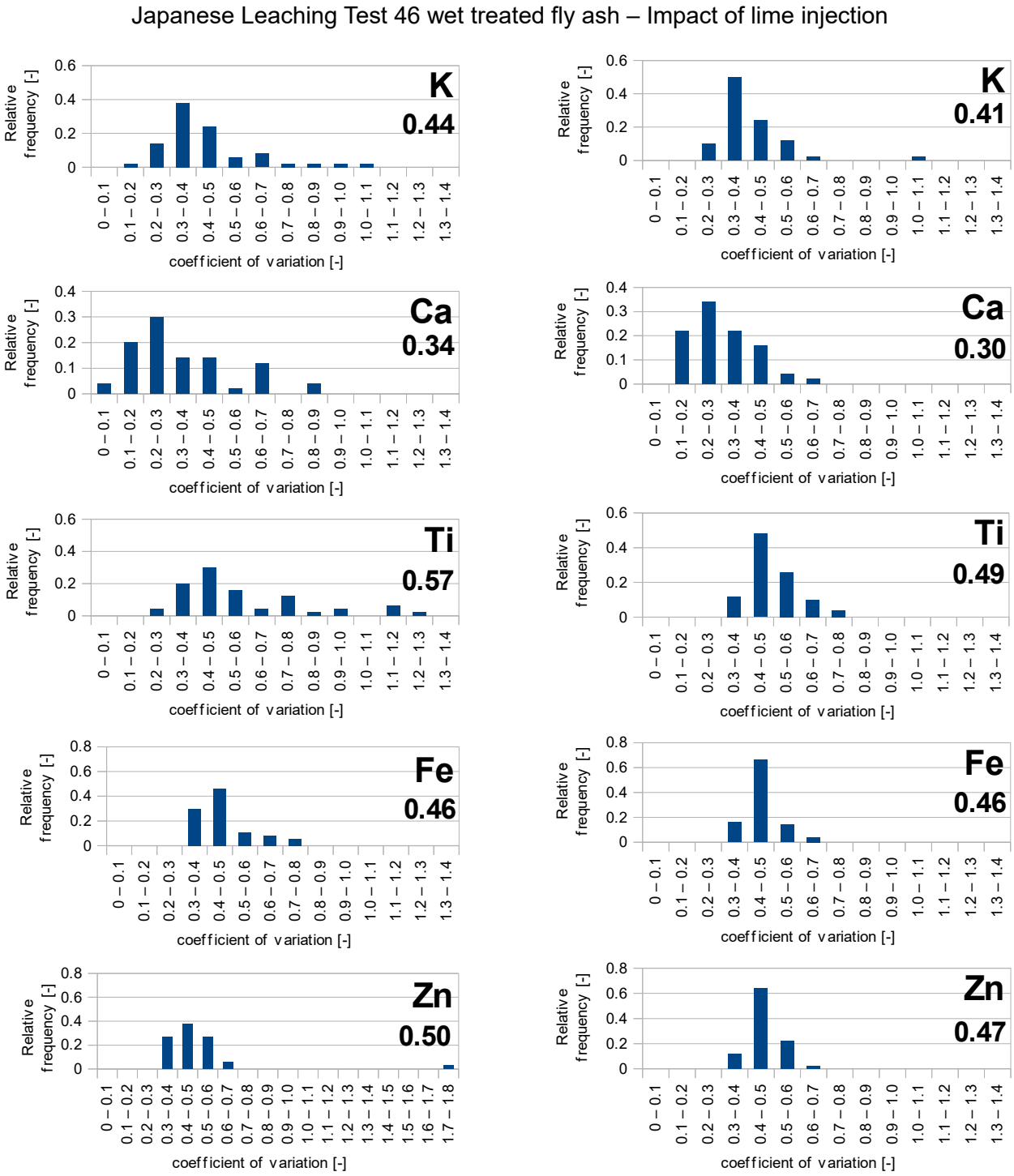

Figure 3.2.6 Major element concentrations on the surface of MSWI fly ash particles after JLT46. Samples were taken from gas cooling tower. Samples on the left side are without and samples on the right side are with lime injection. Values shown in each figure are average CV values of each element.

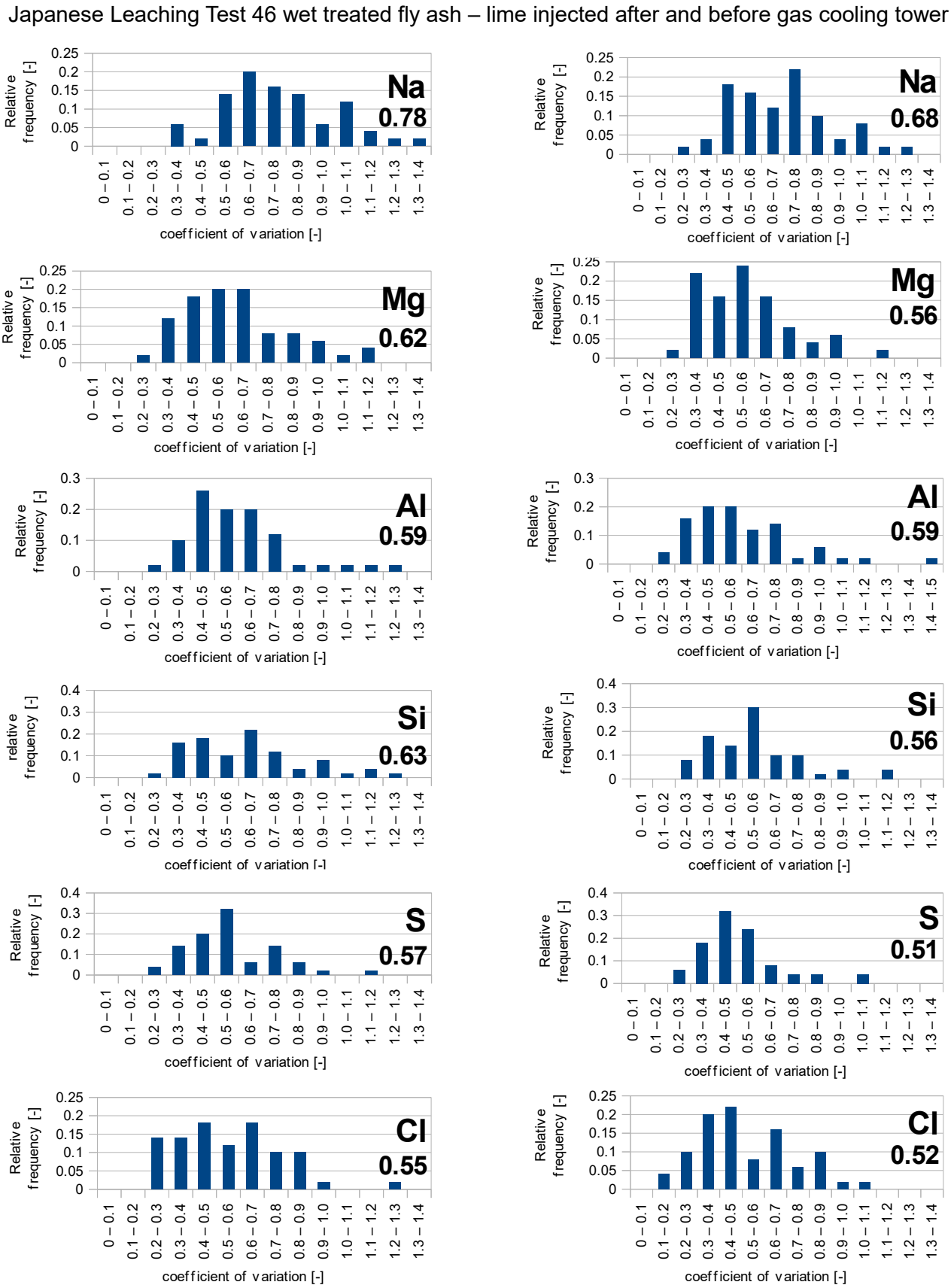

Figure 3.2.7 Major element concentrations on the surface of MSWI fly ash particles after JLT46. Samples were taken from filter-type dust collector. Lime injection was carried out after for left samples and before gas cooling tower for right samples. Values shown in each figure are average CV values of each element.

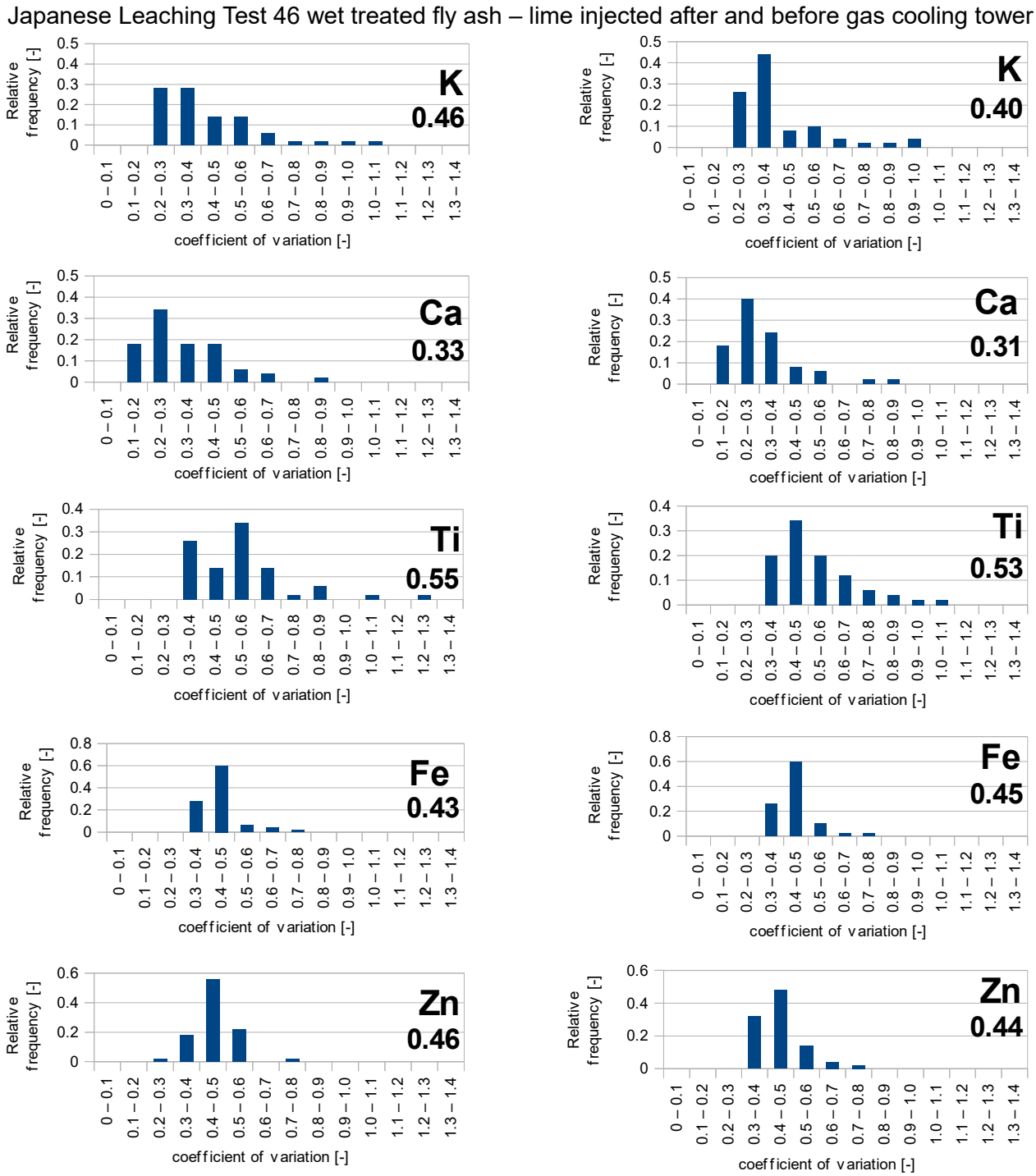

Figure 3.2.8 Major element concentrations on the surface of MSWI fly ash particles after JLT46. Samples were taken from filter-type dust collector. Lime injection was carried out after for left samples and before gas cooling tower for right samples. Values shown in each figure are average CV values of each element.

III) Toxicity Characteristic Leaching Procedure – mid-part of fly ash particles

Impact of lime

The mid-part of municipal solid waste incineration fly ash particles becomes more homogeneous for Calcium and Chlorine but also for the transition metals iron and zinc if lime is injected. Potassium shows the same coefficient of variation for both samples and all other elements are distributed more heterogeneous intra-particle wise when Calcium hydroxide is added into the flue gas stream. All results are shown in figure 3.2.9 and 3.2.10.

Impact of gas temperature at lime injection

The injection point of lime has a relatively small effect. However, it was observable that Chlorine and Titan become more heterogeneous in their intra-particle distribution with lime addition at point 2. No difference in their coefficients of variation were seen for Calcium and Aluminium. The distribution of all other elements become more homogeneous intra-particle-wise. As mentioned before, the biggest change of 0.06 in the coefficient of variation and therefore in homogeneity can be observed for Silicon and Zinc, as shown in figure 3.2.11 and 3.2.12.

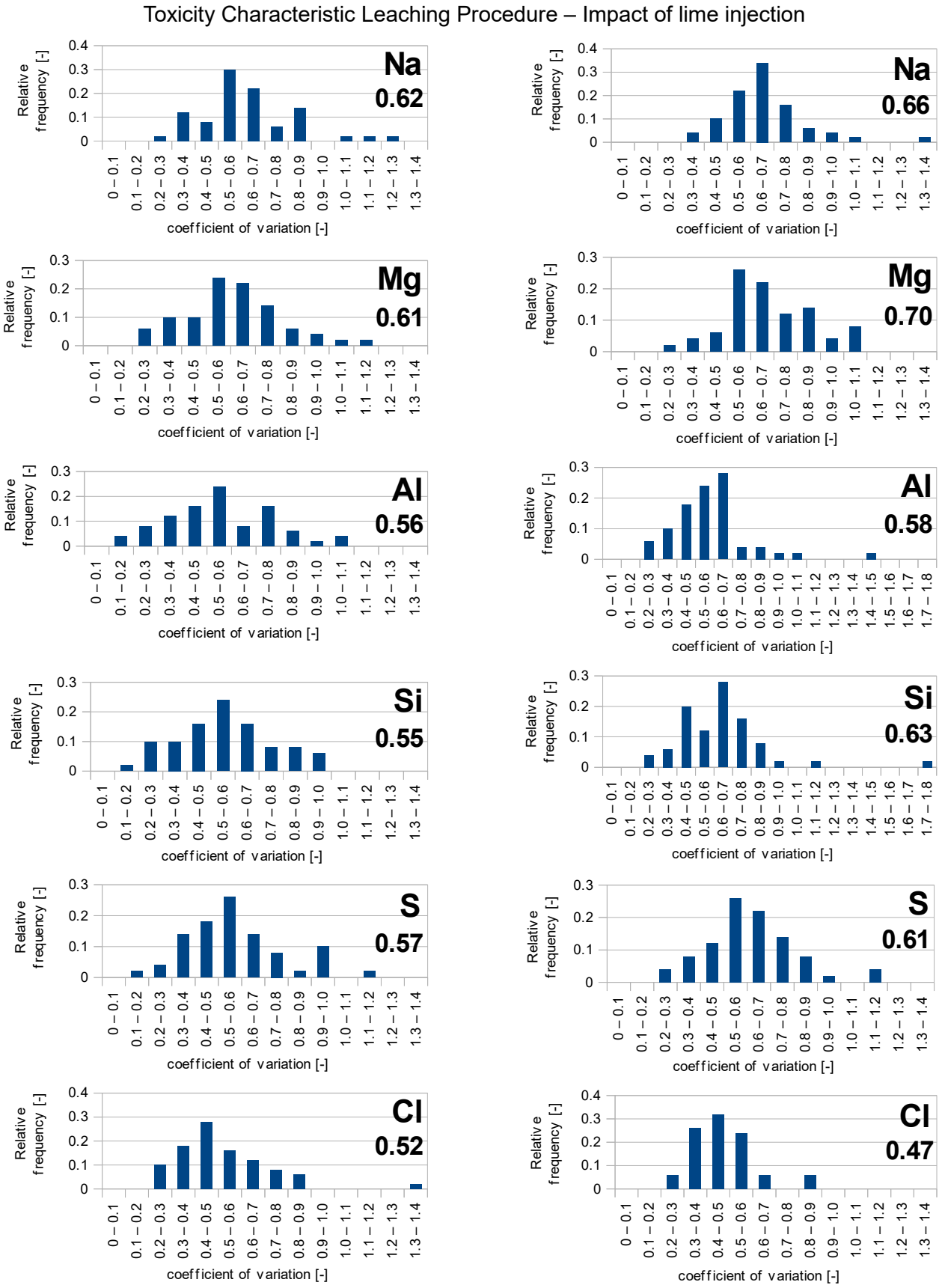

Figure 3.2.9 Major element concentrations of MSWI fly ash particles after TCLP. Samples were taken from gas cooling tower. Samples on the left side are without and samples on the right side are with lime injection. Values shown in each figure are average CV values of each element.

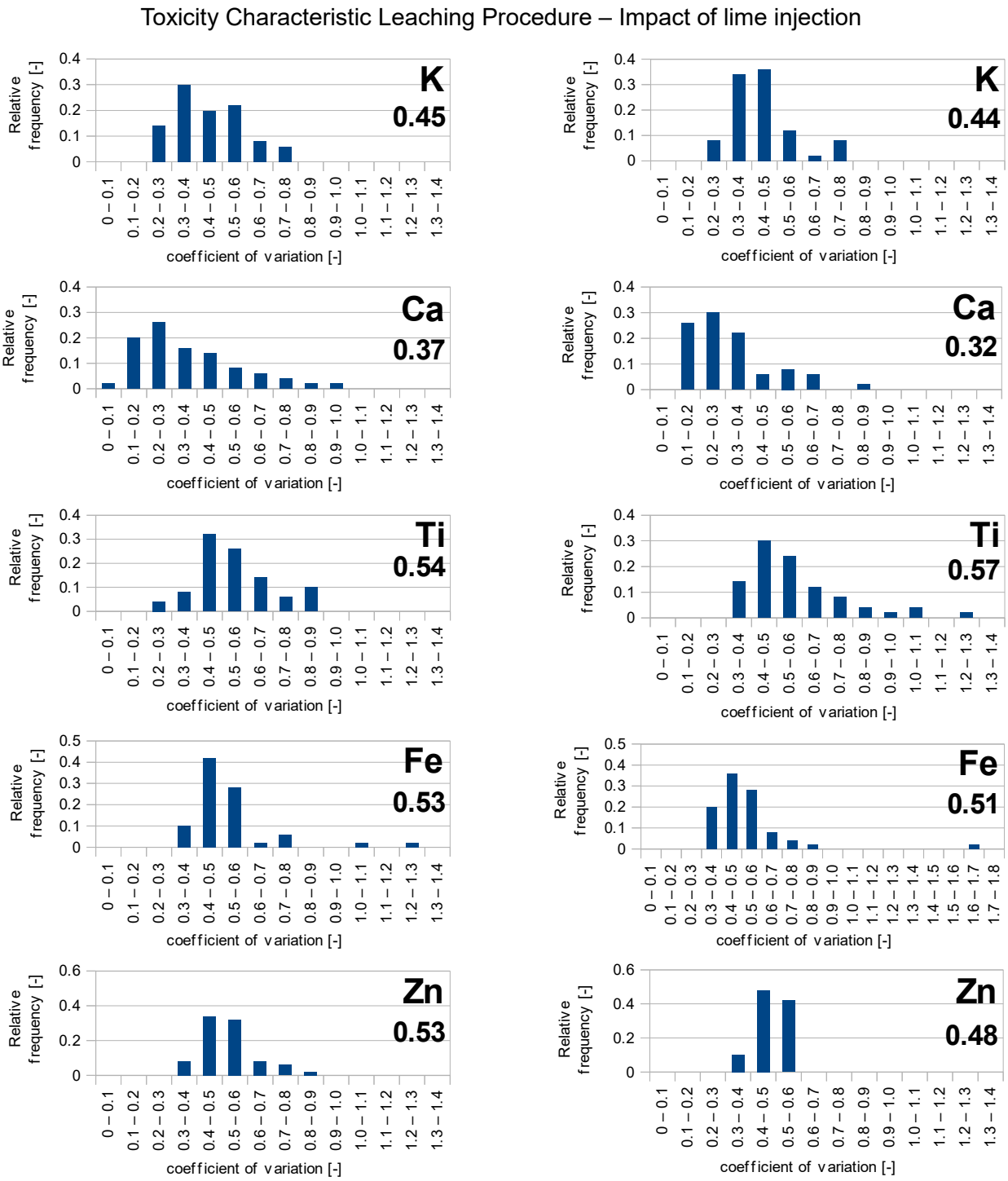

Figure 3.2.10 Major element concentrations of MSWI fly ash particles after TCLP. Samples were taken from gas cooling tower. Samples on the left side are without and samples on the right side are with lime injection. Values shown in each figure are average CV values of each element.

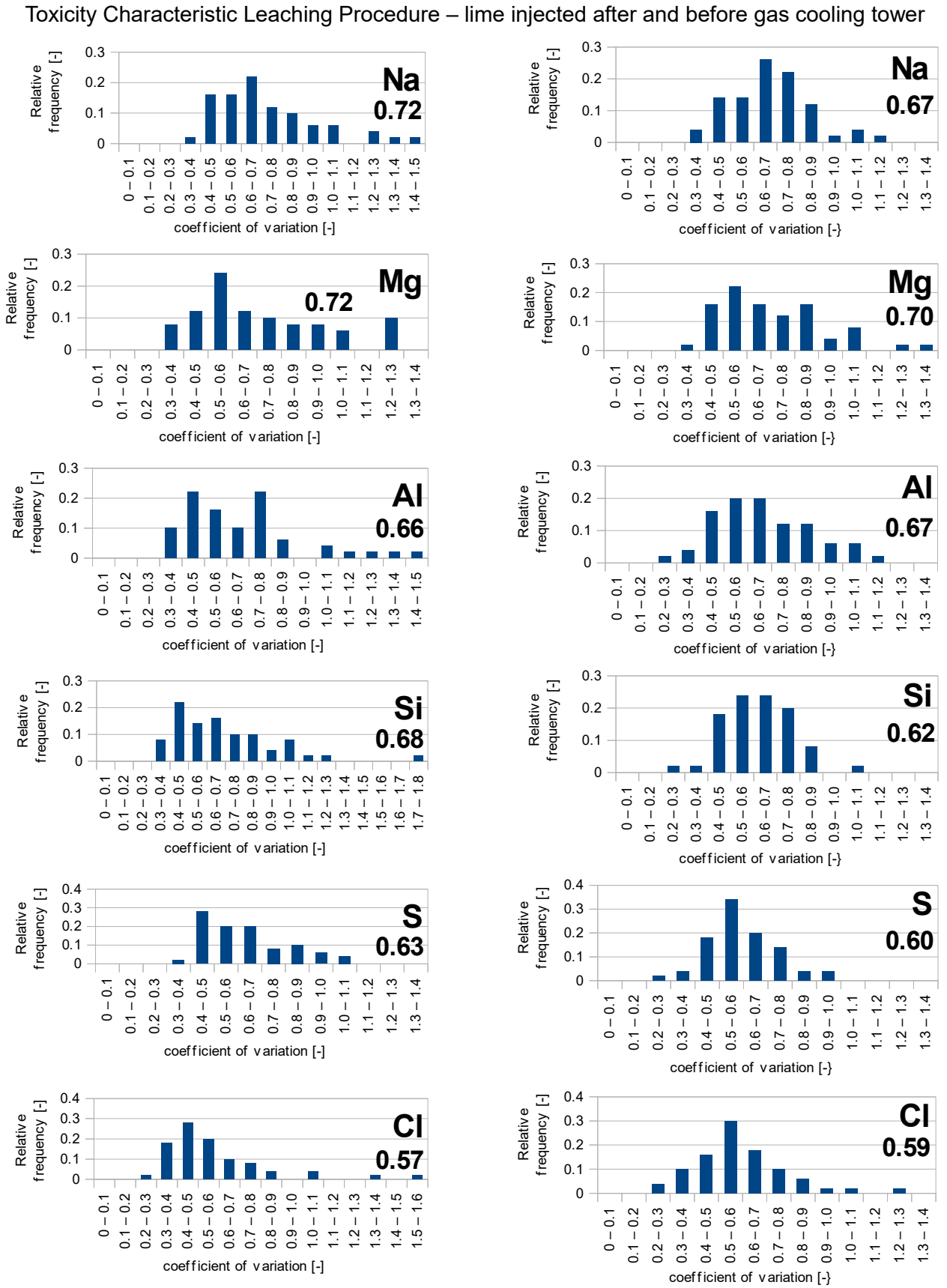

Figure 3.2.11 Major element concentrations on the surface of MSWI fly ash particles after TCLP. Samples were taken from filter-type dust collector. Lime injection was carried out after for left samples and before gas cooling tower for right samples. Values shown in each figure are average CV values of each element.

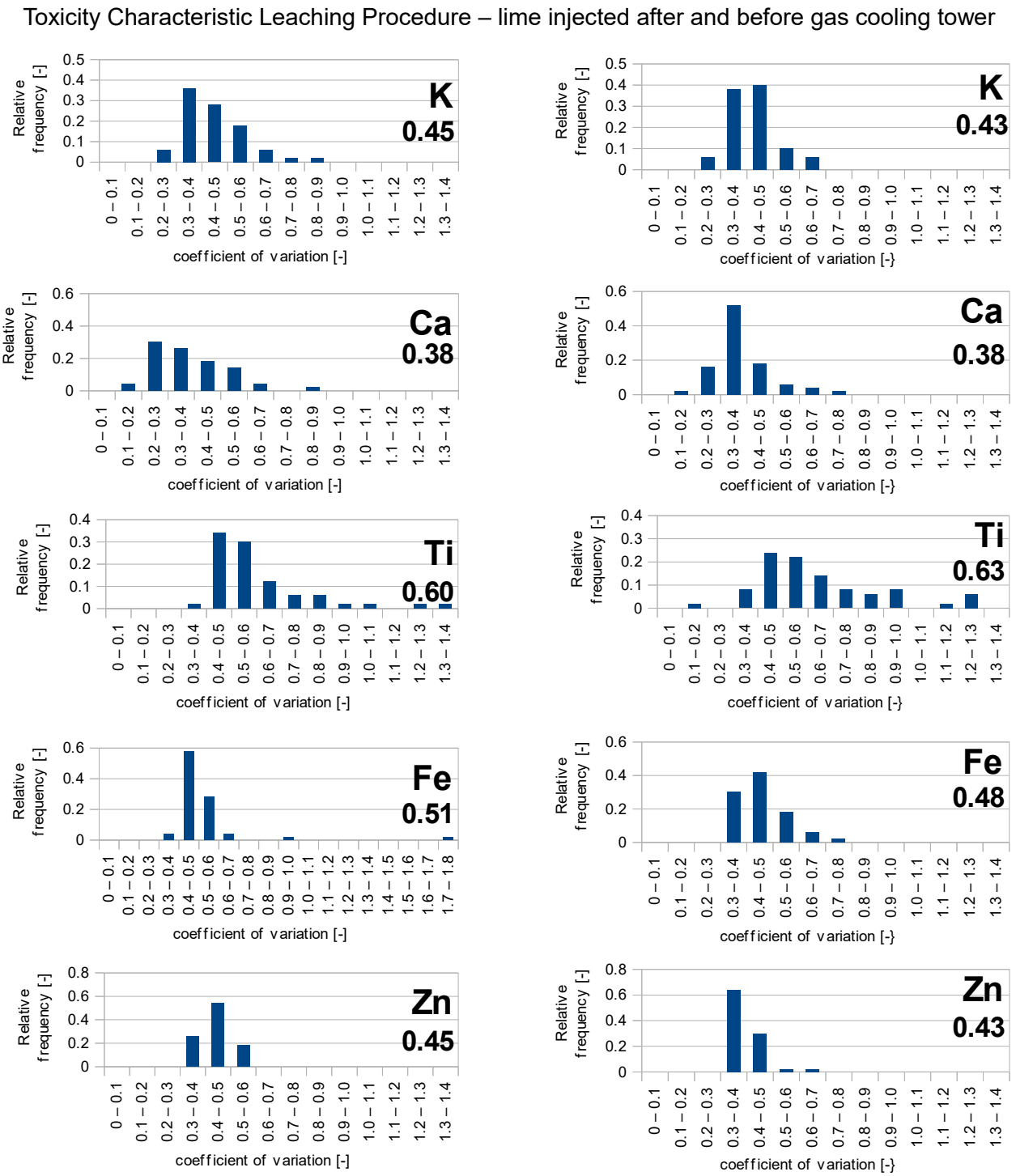

Figure 3.2.12 Major element concentrations on the surface of MSWI fly ash particles after TCLP. Samples were taken from filter-type dust collector. Lime injection was carried out after for left samples and before gas cooling tower for right samples. Values shown in each figure are average CV values of each element.

IV) Japanese Leaching Test 19 – core of fly ash particles

Impact of lime

The results shown in figure 3.2.13 and 3.2.14 lead to the assumption that injected lime can increase the intra-particle homogeneity of the fly ash particle core. Most elements show an increased homogeneity. Sulphur and Potassium become more heterogeneous and no change in intra-particle heterogeneity was observable for Chlorine and Zinc. The increase in homogeneity can be explained by the less frequency of extreme values in the fly ash sample with injected lime.

Impact of gas temperature at lime injection

The results shown in figure 3.2.15 and 3.2.16 show a clear trend regarding intra-particle heterogeneity. All elements increase their intra-particle homogeneity if Calcium hydroxide is injected into the flue gas stream at point 2. The biggest change with 0.10 and 0.09 can be observed for Sodium and Aluminium. On the other side the smallest difference is shown by Sulphur and Calcium with a change of 0.02 of their coefficient of variation.

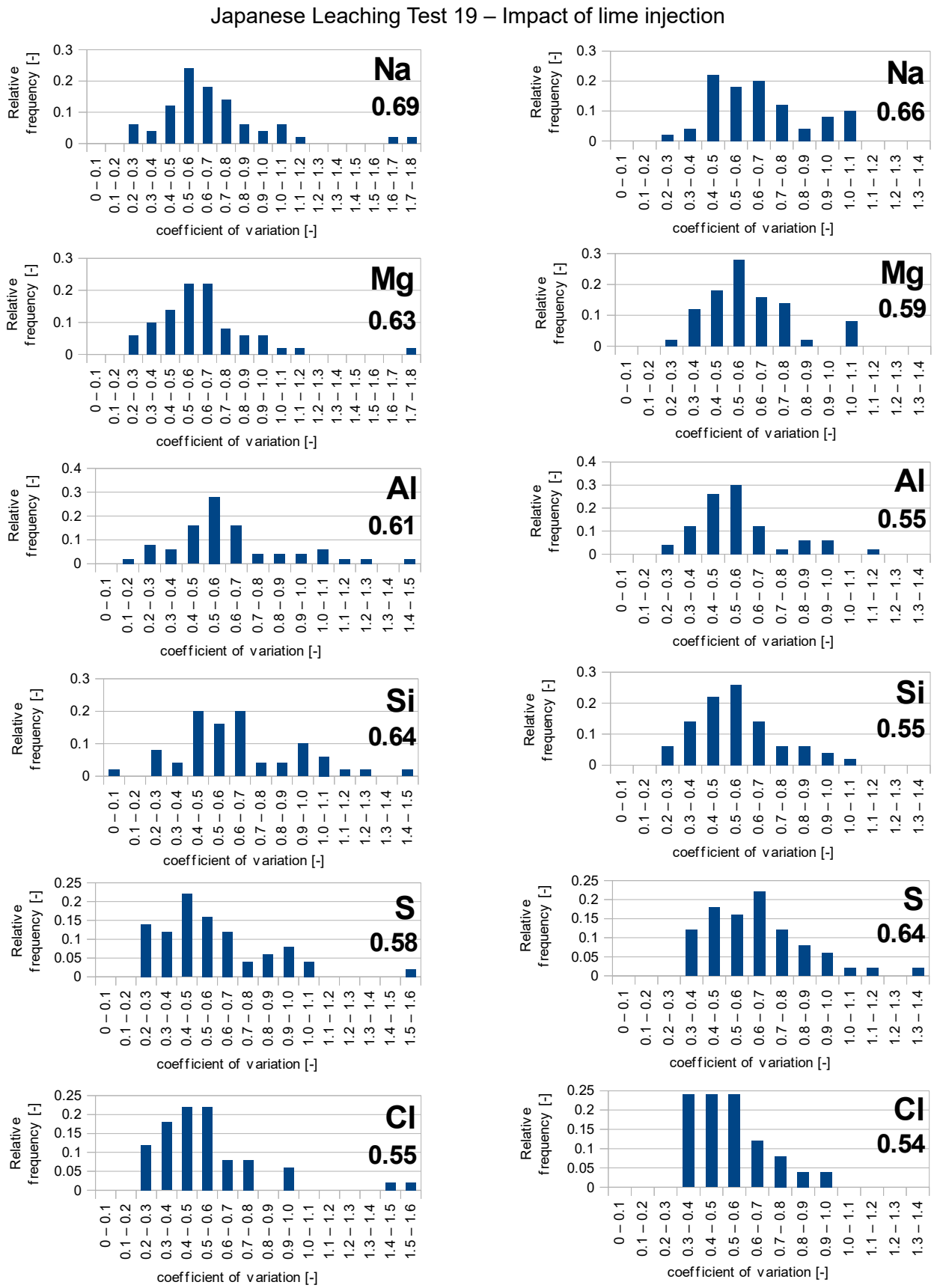

Figure 3.2.13 Major element concentrations of MSWI fly ash particles after JLT19. Samples were taken from gas cooling tower. Samples on the left side are without and samples on the right side are with lime injection. Values shown in each figure are average CV values of each element.

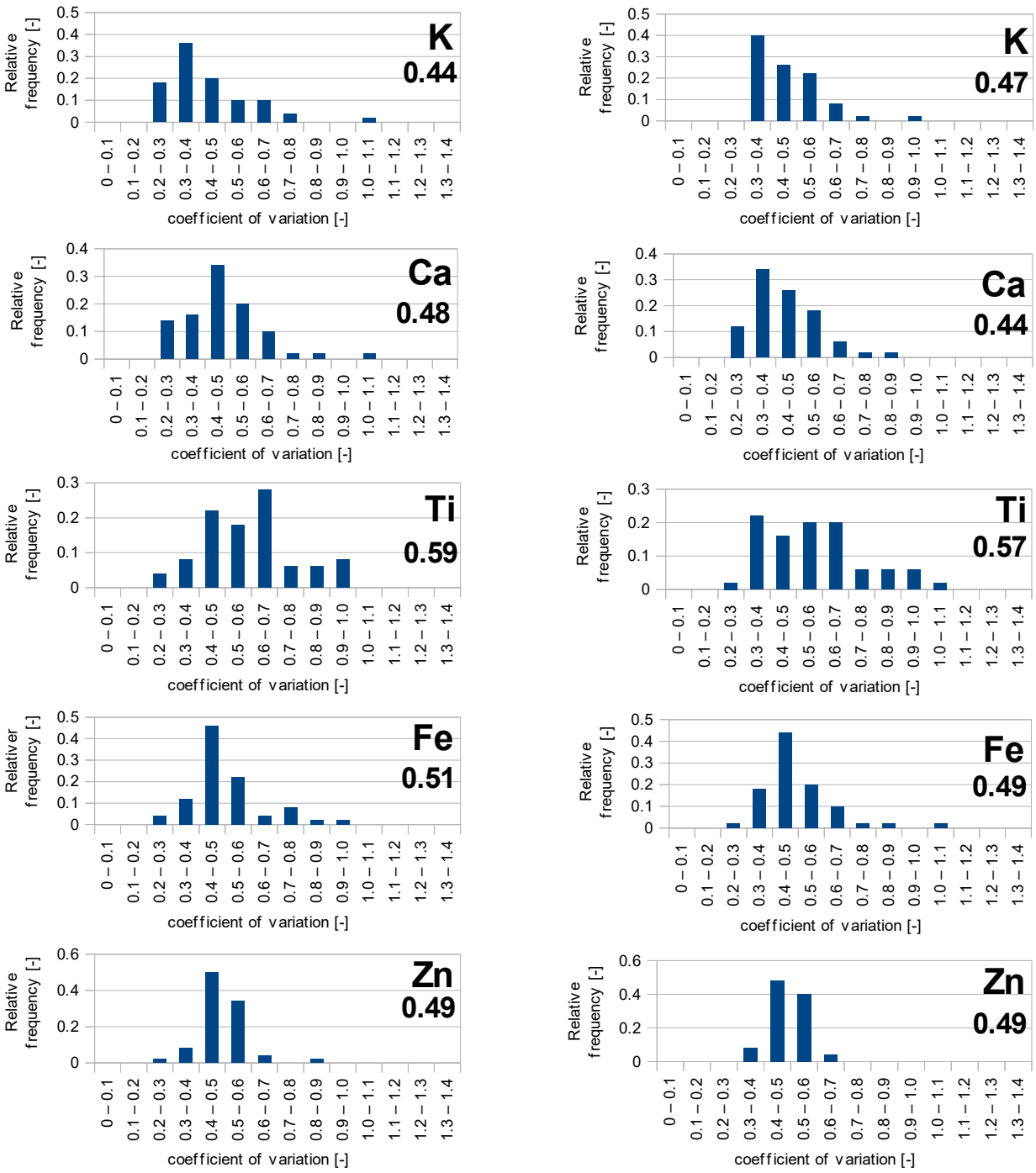

Figure 3.2.14 Major element concentrations of MSWI fly ash particles after JLT19. Samples were taken from gas cooling tower. Samples on the left side are without and samples on the right side are with lime injection. Values shown in each figure are average CV values of each element.

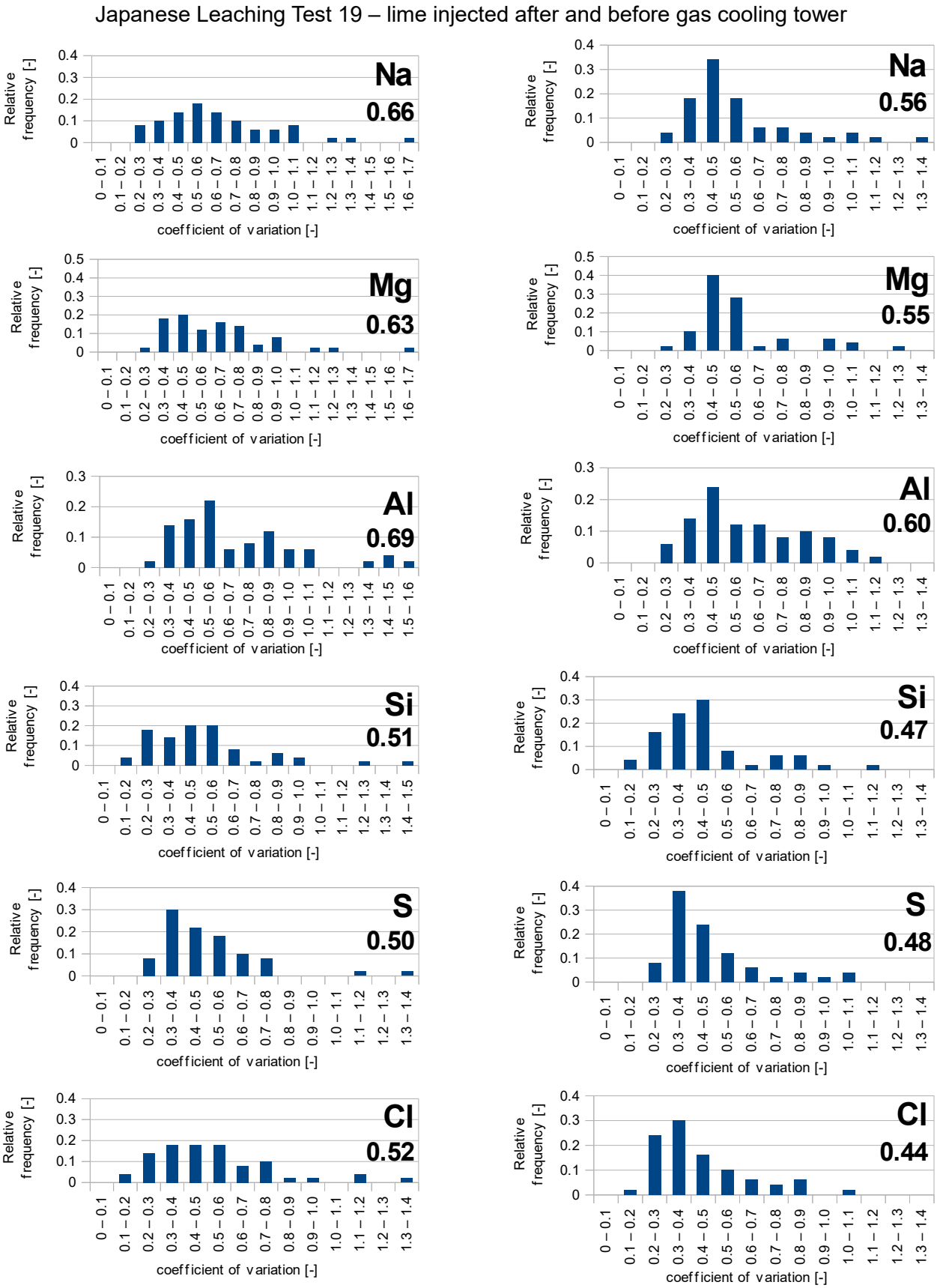

Figure 3.2.15 Major element concentrations of MSWI fly ash particles after JLT19. Samples were taken from filter-type dust collector. Lime injection was carried out after for left samples and before gas cooling tower for right samples. Values shown in each figure are average CV values of each element.

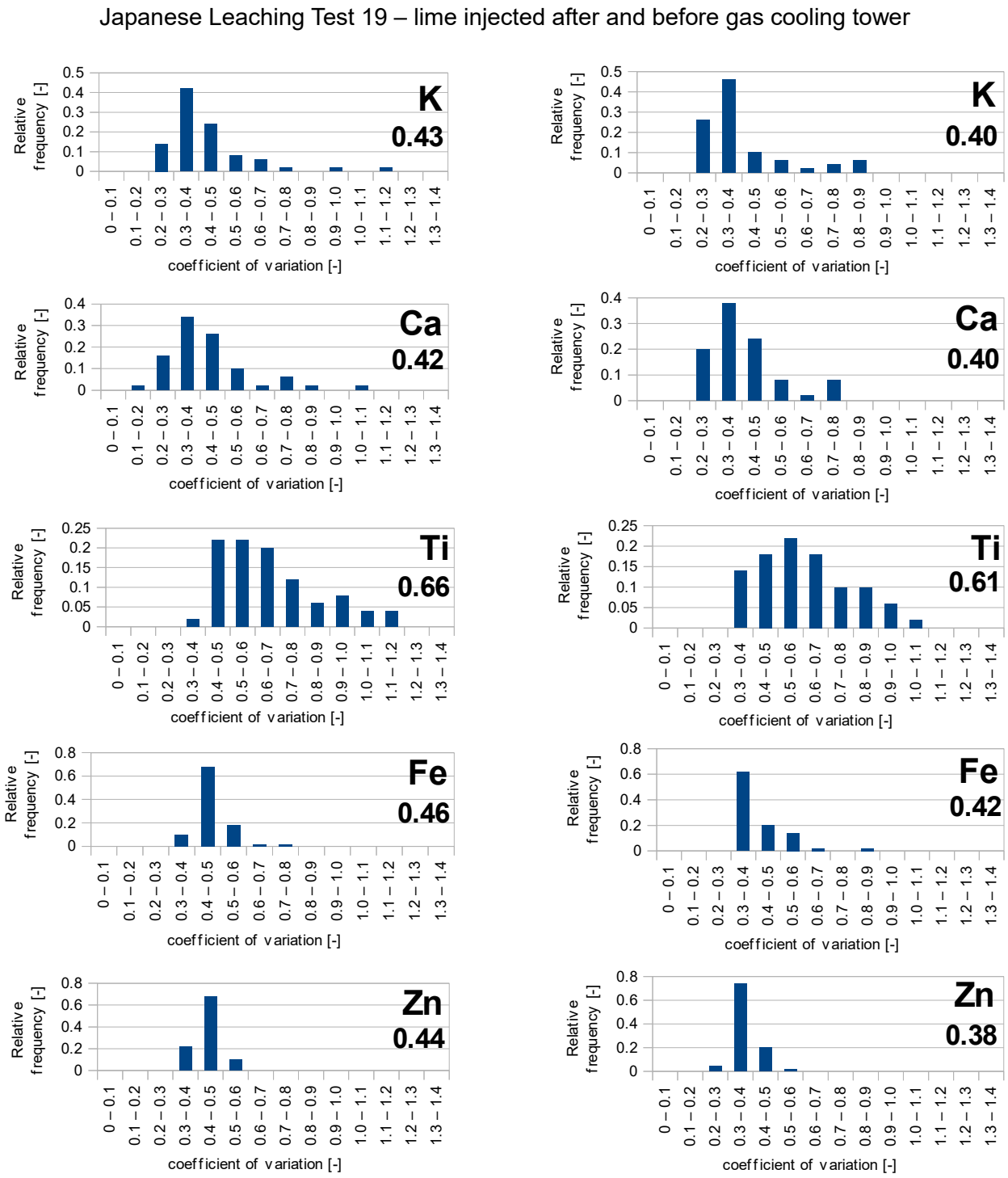

Figure 3.2.16 Major element concentrations of MSWI fly ash particles after JLT19. Samples were taken from filter-type dust collector. Lime injection was carried out after for left samples and before gas cooling tower for right samples. Values shown in each figure are average CV values of each element.

3.3. Single particle analysis vs. bulk analysis

In this study area and line profile analysis was used to investigate single particles. To prove the result's representativeness energy dispersive x-ray fluorescence spectrometry (ED-XRF) was used on a larger sample. Generally ED-XRF is more accurate and more sensible to low amounts. All Elements from sodium to uranium could be observed with XRF analysis. On the other hand SEM/EDX was used at a limit of 10 keV, which results in the incapability of analysing many elements like bromine or lead even though their content might be high enough for observation. Nevertheless, it should be noted that zinc for example has a much higher content as shown by XRF analysis as bromine or lead and still it was not possible to observe zinc in untreated fly ashes with SEM/EDX analysis. Therefore it can be assumed, that all elements which were analysable with SEM/EDX were identified.

Regarding the samples taken from the gas cooling unit the results are shown in table 2. Without injected lime there seems to be quite a difference for most elements. The smallest gap occurs for Al and is 0.26 wt% or 7% but for the rest it is far over 10%. Ca shows the hugest difference of 15.24 wt% or 59% relatively. The results are closer together when calcium hydroxide is injected at point 2. For most elements the difference is around 10%. Magnesium and Potassium are very close and the difference for Calcium is only 4.83 wt% or 10.4%. The hugest difference by percentage is given by Aluminium with 0.78 wt% or 33.5%. It seems possible that lime addition has an effect on particle size and also on particle size distribution. That may cause partly the greater gap between the measurements when no Calcium hydroxide is added. Especially for lime injected samples it seems like the single particle analysis reflects quite well the overall elemental composition of the fly ash particles.

In Table 3 there are the results of the samples derived from air pollution control device and with injection of calcium hydroxide at point 1 and point 2. Both samples seem to be very alike. They show the same gap for Mg (> 0.2wt%), Si (> 0.6wt%) and S (~ 0.5wt%). The difference of Calcium for point-1-injection-samples is less than 3wt% in absolute values and also less than 10% relatively. Point-2-injection-samples show an absolute gap of 4.4wt%. That may lead to the assumption that there might occur slightly different reactions involving Calcium, Chlorine, Potassium and Sulphur.

Overall XRF and SEM/EDX lead to similar results regarding major elements. The difference becomes less when there is lime injection into the flue gases. Although, it should be noted that for elements with minor content XRF analysis is far more preferable.

Table 2: Energy dispersive X-ray fluorescence analysis and comparison with SEM/EDX single particle analysis results of MSWI fly ash taken from gas cooling unit

	Samples taken from gas cooling tower			
	Without lime injection		Lime injection before gas cooling tower	
	XRF	**SEM/EDX**	**XRF**	**SEM/EDX**
Element	Weight percent [wt%]		Weight percent [wt%]	
Ca	41.10	25.86	51.30	46.43
Cl	25.55	32.27	31.60	34.69
K	6.76	10.31	3.54	3.73
Si	5.70	7.71	2.75	3.30
S	3.27	3.84	2.62	3.56
Al	3.46	3.72	1.55	2.33
Mg	1.16	1.73	0.736	0.68
Na	-	11.79	-	4.91
Zn	4.14	-	1.87	-
Ti	3.54	-	1.41	-
Fe	2.78	-	1.37	-
Ba	0.533	-	0.273	-
Eu[1]	0.435	-	0.182	-
Pb	0.319	-	0.138	-
Sb	0.305	-	0.144	-
Br	0.279	-	0.170	-
Sn	0.136	-	0.075	-
Cu	0.132	-	0.058	-
Mn	0.113	-	0.054	-
Sr	0.081	-	0.059	-
Cd	0.027	-	0.016	-
Hg	-	-	-	-
Cr	0.122	-	0.054	-
Zr	0.034	-	0.017	-
Ni	0.013	-	-	-

1 Europium peak is most likely mistaken iron peak

Table 3: Energy dispersive X-ray fluorescence analysis and comparison with SEM/EDX single particle analysis results of MSWI fly ash taken from air pollution control device

	Samples taken from filter-type dust collector			
	Lime injected after gas cooling tower		Lime injected before gas cooling tower	
	XRF	**SEM/EDX**	**XRF**	**SEM/EDX**
Element	Weight percent [wt%]		Weight percent [wt%]	
Cl	48.12	47.24	49.51	50.88
Ca	33.90	31.01	31.23	26.81
K	8.39	7.77	9.08	8.12
S	1.83	2.31	1.69	2.23
Si	1.62	0.98	1.76	1.06
Al	0.813	0.85	0.921	0.92
Mg	0.229	0.51	0.258	0.48
Na	-	8.37	-	9.49
Zn	3.04	-	3.33	-
Br	0.398	-	0.431	-
Fe	0.404	-	0.411	-
Ti	0.363	-	0.378	-
Pb	0.306	-	0.327	-
Sb	0.163	-	0.177	-
Cu	0.098	-	0.102	-
Sn	0.084	-	0.099	-
Eu[1]	0.072	-	0.064	-
Mn	0.029	-	0.027	-
Sr	0.027	-	0.024	-
Cd	0.025	-	0.030	-
Hg	-	-	0.027	-
Ba	-	-	0.085	-
Cr	-	-	0.025	-
Zr	-	-	-	-
Ni	-	-	-	-

1 Europium peak is most likely mistaken iron peak

3.4. Comparing untreated fly ash samples from different plants

The heterogeneity analysis regarding fly ashes from different plants is shown in figure 3.4.1, 3.4.2 and 3.4.3. It should be noted that oxygen was also measured for the second plant data. Therefore the weight percentage values in this study are overestimating the elemental content. In this case oxygen mean content is 29.62 wt% which leads to overestimation of about 30%. Both MSWI plants are operated by the same company and use the same stoker-type incinerator and identical process. The only difference is the composition of the municipal solid waste that is burnt.

The sample investigated in this study shows narrower distributions for most elements and therefore also much lower relative standard deviations. Sodium, Silicon and Potassium are kind of similar distributed. Hence, the sample on the right side in figure 3.4.1, where the results are shown, has a higher inter-particle homogeneity. It also should be mentioned that bestow the fact that both incineration facilities use the same process the fly ash properties seem to vary quite a lot. Same applies for silicon. On the other hand chlorine content of the investigated sample is much higher. The average's difference of about 27wt% may be caused by burning more materials containing chlorine like PVC and other plastics. Calcium is shifted towards higher values in accordance with an increase of the average weight percentage by 10.5%.

Regarding intra-particle heterogeneity the samples show quite the opposite picture as the results in figure 3.4.2 and 3.4.3 show. All elements have a lower coefficient of variation of the green sample except Chlorine. Hence, their intra-particle homogeneity is much higher. The hugest difference occurs for Magnesium, because in the green sample there are many particles with no Magnesium content. Values regarding aluminium content suggest that there are more spots with higher concentration of Aluminium on particles of the green sample. Due to this the coefficient of

variation is higher than one. On the other hand the sample investigated in this study shows a very narrow distribution and the coefficient of variation is roughly halved. Comparing sodium there is a difference of 0.15 in the coefficient of variation for the sample investigated in this study.

To summarize the results there can be quite a difference for fly ash samples. It seems like they depend greatly on the incinerated waste as shown by the data but the process and specific process conditions also have an effect on fly ash composition.

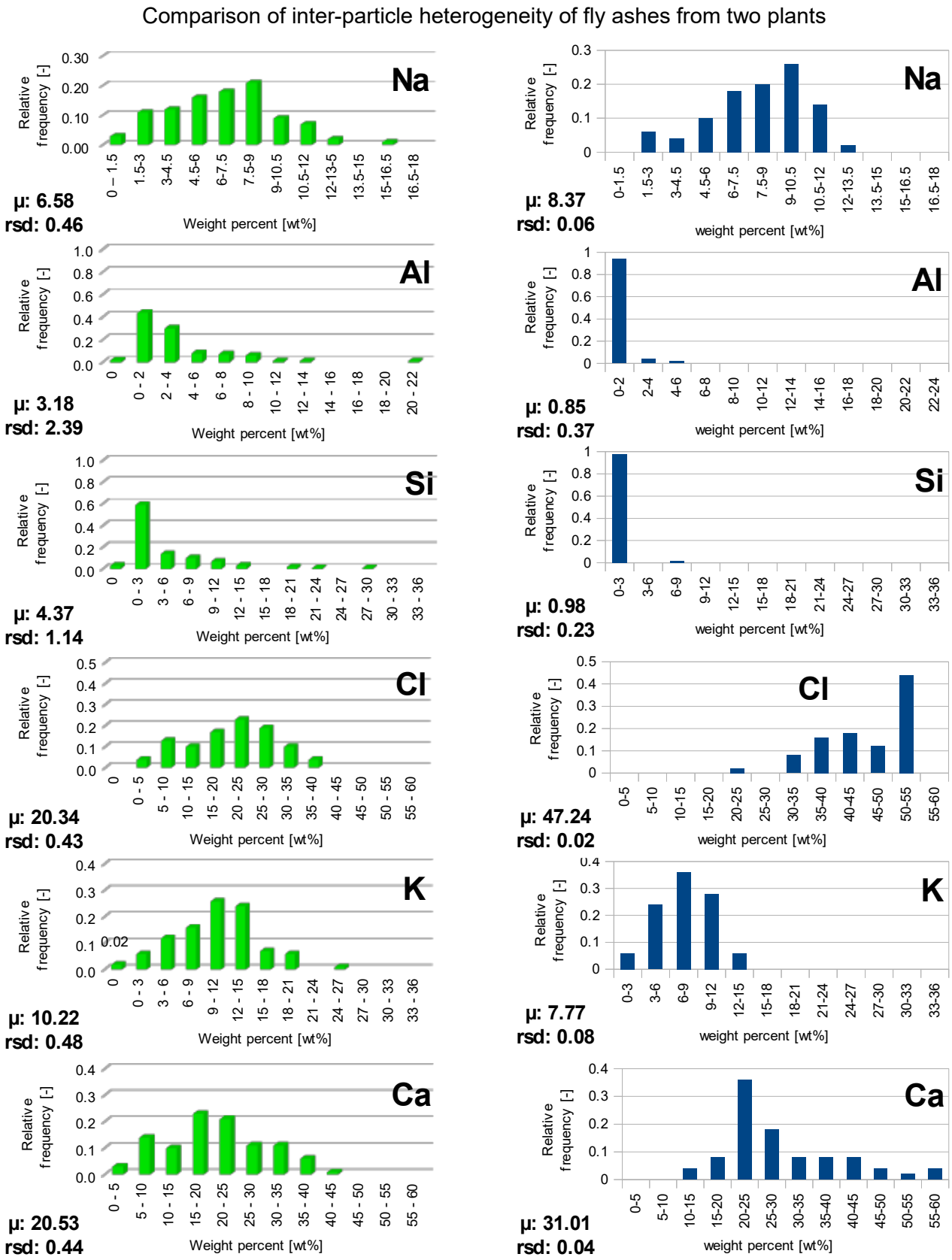

Figure 3.4.1 Major element concentrations on the surface of untreated MSWI fly ash particles derived from filter-type dust collector. Lime injection was carried out after gas cooling tower for both samples. μ: average concentration in weight percent. rsd: relative standard deviation.

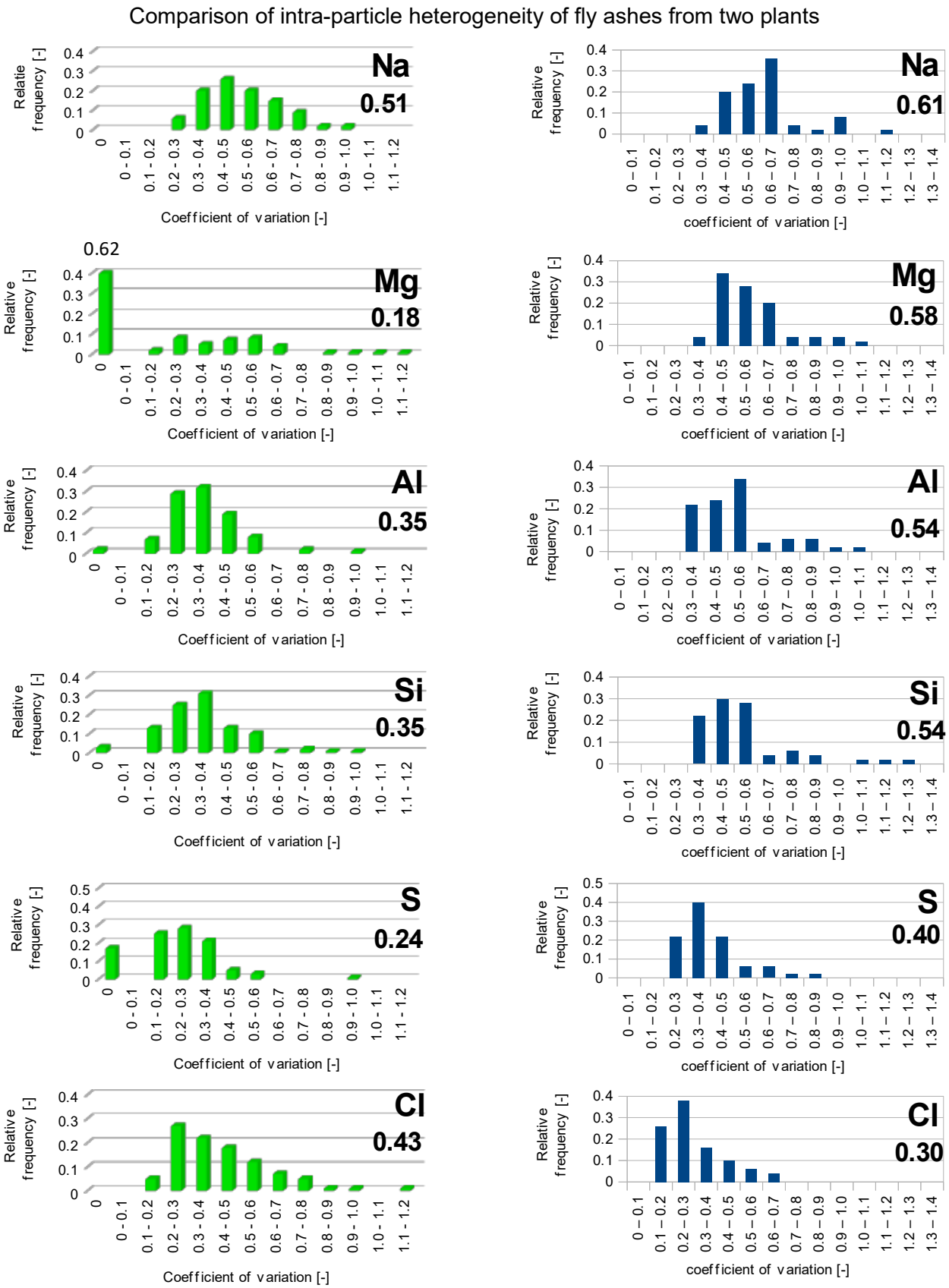

Figure 3.4.2 Major element concentrations of untreated MSWI fly ash particles derived from filter-type dust collector. Lime injection was carried out after gas cooling tower for both samples. Values shown in each figure are average coefficients of variation of each element.

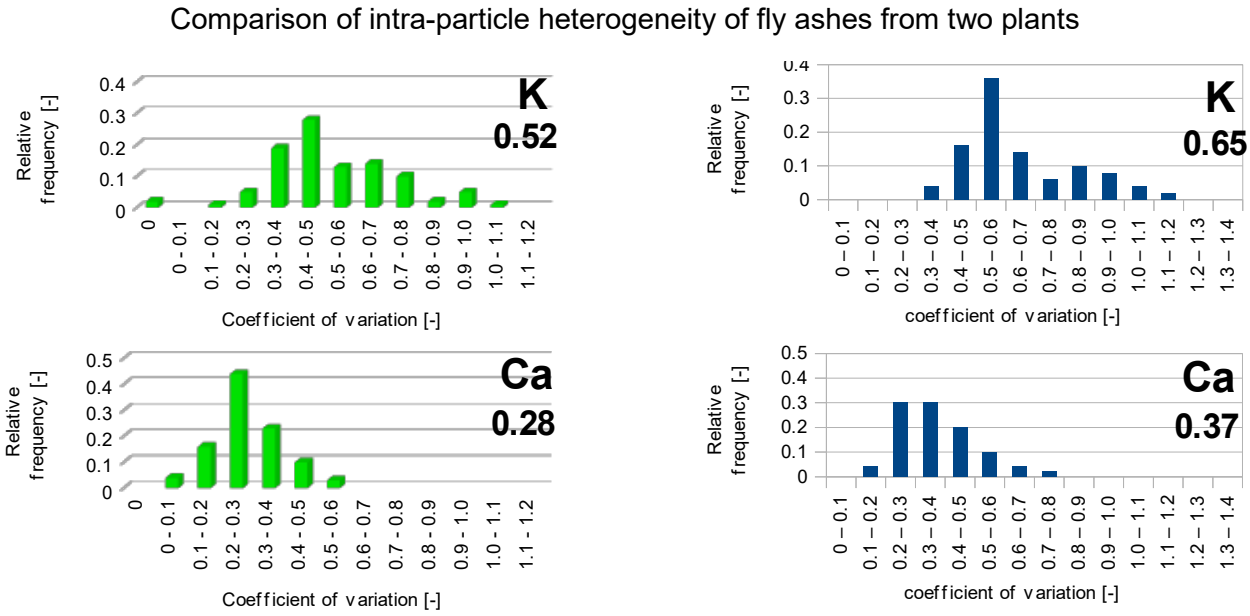

Figure 3.4.3 Major element concentrations of untreated MSWI fly ash particles derived from filter-type dust collector. Lime injection was carried out after gas cooling tower for both samples. Values shown in each figure are average coefficients of variation of each element.

4 Transition metals and their matrix

After carrying out leaching tests transition metals were observable with SEM/EDX method. Hence, for each observed element (Ti, Fe, Zn) 3 particles with high concentration were picked and analysed further. Per particle 3 enriched spots of the analysed metal were averaged and compared to the whole particle. In table 2 the results are shown for titan and iron after “Japanese Leaching Test 19” and in table 3 the observations of zinc after JLT19 and “Toxicity Characteristic Leaching Procedure” (TCLP) are given. Bold values mean higher concentration of given transition metal in those enriched spots than corresponding average values of the whole particle.

The results suggest titan is associated with calcium in first place but also with sodium, potassium and iron. In case of iron it is likely a correlation with magnesium, aluminium, sulphur and titan. Zinc is the only transition metal that can be found after conducting TCLP leaching test. It seems to be very likely that zinc is associated with potassium which is observable for all three particles. There should be some species containing chlorine, titan and iron as well. Less probable are species with sodium, magnesium and silicon which were found only for one particle. It should be noted that all these species are part of the semi-solubles. JLT19 shows most likely a correlation with sodium and aluminium but also with magnesium. That leads to the assumption that insoluble zinc species are associated with any kind of aluminium oxide matrix which also contains most probably sodium and magnesium oxide. Minor association can be found for sulphur, potassium and titan.

Table 4: Composition of titan and iron rich spots after Japanese Leaching Test 19

JLT19	Ti rich [m%]			Fe rich [m%]		
Na	0.83	0.77	**1.76**	2.48	1.78	1.21
Mg	1.42	0.87	1.08	**2.34**	**3.70**	0.40
Al	1.17	1.15	2.55	3.50	**6.85**	1.09
Si	10.88	7.60	17.22	15.21	28.45	5.00
S	1.78	0.75	0.97	**1.86**	0.85	0.49
Cl	5.44	3.48	8.37	11.13	10.51	5.28
K	2.18	0.85	**2.43**	1.30	1.92	0.59
Ca	**19.25**	**29.23**	**7.36**	4.04	5.62	5.44
Ti	51.83	46.76	43.46	3.05	3.38	**13.23**
Fe	0.81	1.95	**6.26**	46.86	26.82	66.71
Zn	6.20	6.75	9.10	16.05	12.19	2.93

Table 5: Composition of zinc rich spots after Japanese Leaching Test 19 and Toxicity Characteristic Leaching Procedure

	JLT19 Zn rich [m%]			**TCLP** Zn rich [m%]		
Na	**3.17**	**4.42**	**2.55**	2.42	1.47	**5.87**
Mg	**1.52**	**1.79**	1.66	1.42	1.91	**3.44**
Al	**14.86**	**15.28**	**7.57**	2.62	2.35	0.46
Si	10.67	19.32	21.72	3.51	4.30	**6.32**
S	0.00	1.06	**1.60**	6.27	5.40	2.53
Cl	9.35	15.39	11.50	**7.89**	5.05	**9.29**
K	1.57	**2.52**	1.92	**2.70**	**2.69**	**3.12**
Ca	2.54	6.94	4.67	21.12	16.02	34.44
Ti	**15.77**	2.84	2.67	**3.40**	**2.90**	0.00
Fe	5.90	4.12	2.97	**4.10**	2.24	**4.00**
Zn	52.20	26.65	43.73	47.50	60.19	39.17

5 Conclusion

In general the addition of calcium hydroxide slurry to the flue gas stream seems to lead to a smaller particle size and therefore a different particle size distribution when compared to the fly ash dropped from the gas cooling unit without lime injection. This is observable even with the naked eye.

By comparing the samples from gas cooling tower the impact of lime injection can be observed. Regarding inter-particle heterogeneity the injection of lime usually triggers a higher inter-particle heterogeneity on the surface of untreated and wet-treated fly ash samples. The mid-part of fly ash samples becomes more inter-particle homogeneous for calcium, chlorine and sulphur. Calcium is injected and should be distributed evenly and the other two are absorbed from the flue gas stream. Hence, most other elements still show a more inter-particle homogeneous distribution without injected lime. Eventually, the inter-particle heterogeneity of fly ash particle cores seem to be only slightly effected by the addition of calcium hydroxide. The comparison of both samples from the filter-type dust collector shows the impact of a different injection point and respectively the injection at different temperatures. There is not much of a difference for untreated fly ash samples. Injection point 2, which is before gas cooling tower, may be leading to a slightly more inter-particle homogeneous surface. Wet-treated fly ash samples also do not show much of a difference between both injection points. The mid-part seems to become more homogeneous for sodium, potassium and the transition metals iron, titan and zinc. This effect becomes even stronger looking at the fly ash particle core. Almost all elements show a higher inter-particle homogeneous distribution when lime is injected before gas cooling. All in all inter-particle heterogeneity appears to be in favour of the modified process with lime injection at point 2 which gives usually narrower distributions and less high values of weight percentage. Nonetheless, less absorption of sulphur

oxides occurring on this process is a drawback. A brief and quantitatively summary of the changes of inter-particle heterogeneity is shown in table 6.

Table 6: a quantitative summary of inter-particle heterogeneity

	higher inter-particle homogeneity	
Untreated FA taken from cooling tower without lime injection	←	Untreated FA taken from cooling tower with lime injection
Wet-treated FA	←	Wet-treated FA
Mid-part of FA	←	Mid-part of FA
FA core	~	FA core
Untreated filter ash with lime injection after cooling tower	~	Untreated filter ash with lime injection before cooling tower
Wet-treated FA	~	Wet-treated FA
Mid-part of FA	→	Mid-part of FA
FA core	→	FA core

Intra-particle heterogeneity is also differently effected by the addition of lime into the flue gas stream. For untreated fly ashes calcium hydroxide increases the intra-particle homogeneity for all elements. Wet treatment shows increased heterogeneity for sodium, magnesium and chlorine. Other elements show no difference or increase their intra-particle homogeneity. The mid-part of observed fly ashes become more homogeneous for calcium, sulphur and chlorine with lime injection. Most other elements decrease their intra-particle homogeneity. The only two elements that decrease their intra-particle homogeneity in the fly ash particle core are Sulphur and Potassium when lime is injected. Eventually, intra-particle heterogeneity of the state-of-the-art process seems to be the best with the lowest coefficients of variation. The process with lime injection at point 2 is still preferable than the one without lime addition. In table 7 is a summary of the results shown.

Table 7: a quantitative summary of intra-particle heterogeneity

	higher intra-particle homogeneity	
Untreated FA taken after cooling tower without lime injection	→	Untreated FA taken after cooling tower with lime injection
Wet-treated FA	→	Wet-treated FA
Mid-part of FA	←	Mid-part of FA
FA core	→	FA core
Untreated filter ash with lime injection after cooling tower	←	Untreated filter ash with lime injection before cooling tower
Wet-treated FA	→	Wet-treated FA
Mid-part of FA	→	Mid-part of FA
FA core	→	FA core

It seems like the injection of calcium hydroxide has adverse effects. Therefore an increase in inter- and intra-particle homogeneity cannot be achieved with one of the investigated processes. On the other side lime injection at higher flue gas temperatures seems to lead to the most homogeneous fly ash particles regarding inter- and intra-particle homogeneity. Maybe this effect becomes stronger at higher gas temperatures than 250°C.

The incinerated waste has a great impact on the composition of fly ashes. Although major core elements Calcium, Aluminium and Silicon remain the same but their ratio changes along with other elements like Sodium, Magnesium, Potassium, Titan, Iron and Zinc accompanying them. The Chlorine content of the fly ashes seems to depend greatly on the amount of incinerated plastics containing Chlorine.

Water soluble species consist mainly of Sodium, Potassium and Chlorine. Compounds leached by Toxicity Characteristic Leaching Procedure (TCLP) are most likely containing Calcium

and Chlorine. Sodium, Calcium, Zinc and Sulphur are those elements which are part of semi-soluble substances leached by Japanese Leaching Test 19 (JLT19). This is in accordance with F. Jiao [13] who found that Zinc is associated with Calcium-species when leached.

Enriched Titan spots show a higher Calcium percentage and in one case engagements with Sodium, Potassium and Iron as well. In case of Iron, higher weight percentages of Magnesium, Aluminium, Sulphur and Titan can be observed as well. After TCLP Zinc appears to be associated with Potassium, Iron, Titan, Chlorine and in individual cases with Sodium, Magnesium and Silicon. Insoluble Zinc-species might consist mainly of Sodium, Aluminium and Magnesium and in minor ratios of Sulphur, Potassium and Titan.

In future it should be focused on investigating the exact heavy-metal-species leached and when it is formed during the incineration process. This understanding is crucial for understanding the leaching process and after that maybe it is possible to avoid the formation of that very species or to trigger formation of an insoluble and stable species which can help to decrease heavy metal leaching. That would lead to a more stable and less hazardous fly ash.

6 References

[1] Bingru Zhang, Weixiao Zhou, Huangpu Zhao, Zhipeng Tian, Fengting Li, Yinan Wu; Stabilazation/solidifacation of lead in MSWI fly ash with mercapto functionalized dendrimer Chelator; Waste Management 50 (2016) 105-112.

[2] Hiroki Kitamura, Takaya Sawada, Takayuki Shimaoka, Fumitake Takahashi; Geochemically structural characteristics of municipal solid waste incineration fly ash particles and mineralogical surface conversions by chelate treatment; Environmental Science and Pollution Research (2016) 23: 734-743. doi: 10.1007/s11356-015-5229-5

[3] Jiang Jianguo, Wang Jun, Xu Xin, Wang Wei, Deng Zhou, Zhang Yan; Heavy metal stabilization in municipal solid waste incineration fly ash using heavy metal chelating agents; Journal of Hazardous Materials B113 (2004) 141-146. doi: 10.1016/j.jhazmat.2004.05.030

[4] H. Ecke, H. Sakanakura, T. Matsuto, N. Tanaka, A. Lagerkvist; State-of-the-art treatment processes for municipal solid waste incineration residues in Japan; Waste Management & Research 2000: 18 41-51.

[5] F. Bodénan, Ph. Deniard; Characterization of flue fas cleaning residues from European solid waste incinerators: assessment of various Ca-based sorbent processes; Chemosphere 51 2003 335-347.

[6] OECD (2018), Municipal waste (indicator). doi: 10.1787/89d5679a-en (Accessed on 26 June 2018)

[7] Rafat Siddique; Use of municipal solid waste ash in concrete; Resources, Conservation and Recycling 55 (2010) 83-91. doi: 10.1016/j.resconrec.2010.10.003

[8] R. V. Silva, J. de Brito, C. J. Lynn, R. K. Dhir; Use of municipal solid waste incineration bottom ashes in alkaliactivated materials, ceramics and granular applications: A review; Waste Management 68 (2017) 207-220.

[9] S. Schlumberger, M. Schuster, S. Ringmann, R. Koralewska; Recovery of high purity zinc from filter ash produced during the thermal treatment of waste and inerting of residual materials; Waste Management Research 25 (2007) 547-555.

[10] Hiroki Kitamura, Astryd Viandila Dahlan, Yu Tian, Takayuki Shimaoka, Takashi Yamamoto, Fumitake Takahashi; Impact of secondary generated minerals on toxic element immobilization for air pollution control fly ash of a municipal solid waste incinerator; Environmental Science and Pollution Research (2018) 25:20700–20712. doi: 10.1007/s11356-018-1959-5

[11] Florian Huber, Dominik Blasenbauer, Ole Mallow, Franz Winter, Johann Fellner; Alternatives Konzept zum Flugaschenmanagement der Stadt Wien; Vortrag: Berliner Konferenz Mineralische Nebenprodukte und Abfälle, Berlin (eingeladen); 20.06.2016 - 21.06.2016; in: "*Berliner Konferenz Mineralische Nebenprodukte und Abfälle*", K. J. Thomé-Kozmiensky (Hrg.); TK Verlag, Neuruppin (2016), ISBN: 978-3-944310-28-2; S. 173 - 183. (only German)

[12] Xiaofei Sun, Jinhui Li, Xiangdong Zhao, Baoli Zhu, Guoliang Zhang; A review on the management of municipal solid waste fly ash in America; Procedia Environmental Sciences 31 (2016) 535-540. doi: 10.1016/j.proenv.2016.02.079

[13] Facun Jiao, Lian Zhang, Zhongbing Dong, Tomoaki Namioka, Naoomi Yamada, Yoshihiko Ninomiya; Study on the species of heavy metals in MSW incineration fly ash and their leaching behavior; Fuel Processing Technology 152 (2016) 108-115. doi: 10.1016/j.fuproc.2016.06.013

[14] A. Purgar, F. Winter, D. Blasenbauer, S. Hartmann, J. Fellner, J. Lederer, H. Rechberger; Main drivers for integrating zinc recovery from fly ashes into the Viennese waste incineration cluster; Fuel Processing Technology 141 (2016) 243-248. doi: 10.1016/j.fuproc.2015.10.003

[15] F. Winter, J. Weber, D. Blasenbauer, A. Purgar, F. Huber, J. Fellner; Characteristic Behaviour of Heavy Metals in Vienna's Waste Incineration Cluster;

[16] Franz Winter, Jakob Weber; The Importance of Waste Incineration for Urban Mining; Preceedings of the European Combustion Meeting 2017

[17] Aurore De Boom, Marc Degrez; Combining sieving and washing, a way to treat MSWI boiler fly ash; Waste Management 39 (2015) 179-188.

[18] Hiroki Kitamura, Astryd Viandila Dahlan, Yu Tian, Fumitake Takahashi; Individual and inter-particle heterogeneity analysis of the surface and inner matrices of chelate-treated MSWI fly ash particles employing water extraction; 5th International Conference on Sustainable Solid Waste Management (Athen, Greece, 21-24th June 2017).

[19] Jouko Lavta-Somppi, Mikko Moisio, Esko I. Kauppinen, Tuomas Valmari, Petri Ahonen, Unto Tapper, Jorma Keskinen; Ash Formation during fluidized-bed incineration of paper mill waste sludge; Journal of Aerosol Science Vol. 29, No. 4, pp. 461-480, 1998.

[20] K. Mäntykoski, J. Paasivirta, E. Mannila; Combustion Products of Biosludge from Pulp Mill; Chemosphere Vol. 19, Nos. 1-6, pp. 413-416, 1989.

[21]

[22] Scheme of a municipal solid waste incineration plant: http://www.takuma.co.jp/english/product/msw/images/stoker_msw/img3.jpg (3rd November 2018)